Pre-Processing techniques and their robustness to channel estimation errors

Group: 08gr1113
Philippe Bouquet
François Ortolan

Supervisors:
Persa Kyritsi, Elisabeth De Carvalho

10th semester
February 2008 to June 2008

Contents

Electronic Systems
Division of Telecommunications
Niels Jernes Vej 12
Telefon 96 35 80 80
http://kom.aau.dk/

Title:
MIMO pre-processing techniques and their robustness to channel estimation errors

Theme:
MIMO, Pre-Processing
CSI imperfection, AMC
Water-filling,Eigenmode

Projectperiod:
February 2008 - June 2008

Project group:
08gr1113

Members:
Philippe Bouquet
François Ortolan

Supervisors:
Persa Kyritsi
Elisabeth De Carvalho

Copies: 3

Pages in report: 91

Pages in appendices: 4

Supplement: CR-ROM

Printed June 4, 2008

Abstract:

The goal of this project is to determine the effect of an imperfect channel estimation on the pre-processing schemes efficiency. Pre-processing is an unavoidable concern in MIMO transmission, especially on the pre-processing techniques investigated: Eigenmode-transmission, Water-filing, and Adaptive modulation and coding. The impact of noise and Doppler CSI imperfection on MIMO systems are investigated using mathematical models and computer simulations. The results are showing that the quality of the estimation channel is crucial for multi-antenna systems.

List of Abbreviations

$ZMCSCG$	Zero-Mean Circularly Symmetric Complex Gaussian
Tx	Transmitter
Rx	Receiver
$TxRx$	Transmitter-Receiver
ISI	Inter Symbol Interference
SNR	Signal to Noise Ratio
SNR_i	Instantaneous Signal Noise to Ratio
BER	Bit Error Rate
SER	Symbol Error Rate
LOS	Line of sight
PDF	Probability density function
$SISO$	Single Input Single Output
$MIMO$	Multiple Input Multiple Output
CSI	Channel State Information
UL	Uplink
DL	Downlink
AMC	Adaptive Modulation Coding
$AWGN$	Additive White Gaussian Noise
PSK	Phase Shift Keying
$BPSK$	Binary Phase Shift Keying
$QPSK$	quadrature phase-shift keying

List of Symbols

Propagation

$y(t)$	Signal received at terminal
A	Signal amplitude also called envelope
$\phi(t)$	Signal phase
F_c	Original frequency
F_d	Maximum Doppler shift
σ_t	Delay spread
Ts	Symbol time
B_c	Coherence bandwidth

Channel Model

Lower case letters are used for functions in the time domain
Upper case letters are used for functions in the frequency domain
Vectors are written with an arrow, e.g. $\vec{x}$
Matrices with capital letters, e.g. $\mathbb{H}$

$h(t,\tau)$	Impulse response function
$H(f,t)$	Transfer function
f	Frequency
t	Time
$n(t)$	Noise added at the receiver
$s(t)$	Stream
$x(t)$	Sent signal
$y(t)$	Received signal
$z(t)$	Post-process received signal
σ_n^2	Noise variance

$\delta(.)$	Dirac impulse
τ	Delay
$\mathbb{H}$	Channel matrix
Ps_{avg}	Average probability of symbol error for some diversity schemes
A_g	Array gain
$Y(f)$	Fourier transforms of $y(t)$
$X(f)$	Fourier transforms of $x(t)$
N_{Tx}	Number of emitting antennas
N_{Rx}	Number of receiving antennas
$\mathbb{H}$	Channel Matrix
N_d	Diversity order
$\vec{x}$	Input signal
$\vec{n}$	Added noise
SNR_i	Instantaneous SNR
SNR_{avg}	Average SNR
$SNR_{\Sigma avg}$	Average combined SNR

Eigenmode-based pre-processing schemes

λ	Scalar defined as an eigenvalue
$\mathbb{U}$	Complex unitary matrices with sizes N_{Tx} x N_{Tx}
$\mathbb{V}$	Complex unitary matrices with sizes N_{Rx} x N_{Rx}
Λ	Real non-negative singular values of size $min(N_{Tx}, N_{Rx})$
$\mathbb{W}$	Weight matrix
$\mathbb{J}$	Weight matrix
λ_k	Eigenvalue of a subchannel
P_k	Power allocated to a subchannel
P_t	Total power
$1/v$	Waterline

CSI estimation errors and Modeling

$\sigma_{\mathbb{H}_{error}}$	Standard deviation of the CSI error
$\mathbb{N}$	is a ZMCSCG matrix of dimensions N_{Tx} x N_{Rx} with a variance of 1.
$\hat{\mathbb{H}}$	Channel estimated
$\hat{\mathbb{H}}_{no}$	Channel estimated with only noise error
$\hat{\mathbb{H}}_{do}$	Channel estimated with only Doppler error
L	Length of the training sequence
T	Quality of the channel estimation
$SNR_{\mathbb{H}_{est}}$	Channel quality expressed in dB
ρ	Correlation coefficient between $\mathbb{H}$ and $\hat{\mathbb{H}}$
f_{dmax}	Maximum Doppler frequency
J_o	Bessel function
u	Receiver speed
c	Speed of light
δ_l	Distance traveled between two measures

Simulations

P_b	Bit error probability
P_M	Symbol error probability
Q	Q function
$\frac{\epsilon_b}{N_0}$	Energy per bit to noise power spectral density ratio
M	Constellation size
k	modulation order
N_{bits}	Total number bits sent
δh_i	Misestimation of the channel for one stream

Preface

This report is the document for our 10th semester project in Mobile Communication, carried out at the department of Electronic Systems at Aalborg University, Denmark. It is addressed to our project supervisors, teachers and students who are interested in the impact of Channel State Information errors in MIMO communications. The thesis investigates how the CSI imperfections can impact the performance of MIMO pre-processing schemes. The study is based on computer simulations and theoretical analysis. The reader is expected to know the basics of wireless telecommunications. The aim of the report is to document the work performed during the 10th semester project. Concerning the report itself, it is composed of two main parts, the theoretical part and the simulations results. *Fig* marks pictures with two numbers, like *1.3*, the first number referring to the chapter and the second one corresponding to the place of the picture in the chapter. For the tables, the term *Fig* is replaced by *Table*, with two numbers, which follow the same rules as the pictures. The numbers in square brackets [1] denote the literature or website reference of a picture or scheme or table. All these references are listed at the end of the report, sorted by order of appearance. Appendices have been included to clarify some of the basic aspects at the end of the report.

We would like to thank our project supervisors, Persefoni Kyritsi and Elisabeth de Carvalho for there help, patience and support throughout the whole project.

François Ortolan   Philippe Bouquet

Aalborg, June 4, 2008

Chapter 1

Introduction

Current wireless systems operate with a centralized structure: a central access point (base station for cellular wireless systems) communicates information to the user located within its coverage area. To do so, they sometimes use information acquired from the users. This information takes on many forms and is commonly referred to as channel state information (CSI). CSI relates to the quality of the channel, e.g. the Signal to Noise Ratio (SNR). However, such a structure has drawbacks: CSI is acquired with a process that is naturally impaired by noise and this only happens periodically so it is not always up to date because of user mobility. The purpose of our project is to investigate how detrimental this noisy and outdated CSI is on the efficiency of pre-processing schemes. Two types of channel estimation error are investigated: noise during the channel estimation process and the Doppler effect due to receiver mobility.

The project is focused on *Multiple-Input Multiple-Output (MIMO)* communication systems. MIMO wireless channel promises significant gain performance over that offered by the conventional single-antenna systems. Unfortunately, for such systems, the CSI is indispensable. The study is based on three pre-processing schemes : *Eigenmode-transmission* which is specific to multi-antenna systems and vital for MIMO, and two other techniques called *Adaptive Modulation and Coding (AMC)*, and *Water-filling*. The impact of the imperfect CSI on pre-processing schemes is evaluated using computer simulations.

The first chapter states our project delimitations where are mentioned the assumptions we made and the directions we chose. Then, important notions regarding the signal's propagation, the various communication systems and CSI and their estimation are reviewed. In a third chapter are present the pre-processing schemes we used and, lastly, their results as they are tested with a different knowledge of the CSI in the simulations chapter.

Chapter 2

Project delimitations

The goal of our project is to show the impact of a misestimated channel on pre-processing schemes. We had carte blanche concerning the method(s) we would use to introduce errors. A tremendous amount of systems could have been studied. However, as our project was limited to a period of six months, we decided to focus our investigation on what seemed the most interesting with respect to our basic knowledge. The following sections present and explain our choices in details.

2.1 System configuration

The system configuration is determined by the number of antennas. The system chosen is a MIMO, a structure composed of multiple antennas at each transceiver. MIMO drew our attention due to the variety of processing methods which have been recently developed in this domain, allowing new communications perspectives, such as increasing the coverage (beamforming), increase the capacity or improve the link quality.

2.2 Pre-processing

Another aspect making MIMO interesting is the difference in the use of processing schemes from a Single Input Single Output (SISO) case. Classical schemes are also used but some more advanced schemes are essential to perform multi-antenna transmission. Each application enumerated below uses a different scheme which unfortunately cannot be simultaneously used with any other one. Consequently, we have decided to focus our work on a specific application of MIMO prone to increase the capacity.

One of the technique used to multiplex various streams over several antennas is the Eigenmode-Transmission. As most of the pre-processing schemes, it requires the knowledge of the channel at the transmitter. In order to increase the capacity as a function of the SNR, we have also coupled the Eigen-transmission with a mechanism called AMC. AMC is a pre-processing technique which uses the measured values of instantaneous SNR of each link to choose the modulation to use for each stream. Instantaneous SNR is retrieved from the channel estimated.

An intelligent way to improve AMC is to use another technique of pre-processing named Water-filling. It also uses the SNR measured to decide how to allocate power over links. More power is allocated to strong links and if the quality of the link is really poor, there is no power allocated at all. Water-filling is really interesting for AMC because it allows to obtain better SNR and consequently to use higher modulation orders.

As explained before, our goal is to maximize the capacity, but we also have to take into account the quality of the transmission. To achieve a good adaptive modulation, a Bit Error Rate (BER) threshold has to be set. In order to respect this threshold, we have decided not to transmit streams below a certain level of SNR. Indeed, even with the lowest modulation order, we can not achieve such a low BER for low values of SNR. This non-transmission can also be considered as a pre-processing.

Thus, the pre-processing techniques used are :

- Eigenmode transmission
- AMC (with no transmission under a certain SNR)
- Water-filling

2.3 Modulation

A large variety of modulations can be used. The main goal of the project is to study preprocessing schemes; the modulations used are not the main concern. Therefore, PSK (Phase Shift Keying) modulation has been chosen for convenience. The PSK constellation is uniquely based on phase components, the amplitude of the signal is not taken into account in the demodulation decision.

2.4 Fading

The fading model chosen is Rayleigh fading, one of the most common in communications domain. This model represents multipath transmissions without any Line of Sight (LOS).

2.5 Wideband/Narrowband

A major decision is to define the symbol time, in order to know in which context the transmission is performed, according to the channel properties. For convenience, the project is not taking into account Inter Symbol Interference (ISI), thus we assume we are in a Narrowband context. The Wideband and Narrowband situations are presented in details in Appendix A.1.

Chapter 3

Background

This aim of this chapter is to present the telecommunications context of the project. The context in telecommunications is effectively important, since it determines which model should be chosen to fit reality as good as possible. Furthermore, knowing the context, some physical aspects can be voluntary neglected for simplification purposes as presented in the previous chapter.

The topics discussed are the theoretical basis of the project. The first section deals with propagation phenomena. The second section covers SISO and MIMO communication systems. Finally, the notion of channel state information and its estimation are introduced.

3.1 Propagation

The propagation channel has a strong influence on the communication system performance. The knowledge of its properties is fundamental to design efficient wireless systems. This section presents the main phenomena involved in electromagnetic propagation and the mathematical representation for such phenomena. The signal perturbations can be represented in the spatial, temporal and frequency domain.

In wireless communications, the signal can be represented as an infinite number of rays propagating between the emitter and the receiver, using different paths. The receiver sees the signal as the sum of all the contributions of the multipath components. Each ray is influenced by several electromagnetic perturbations such as reflection, diffraction and scattering, illustrated in Figure 3.1.

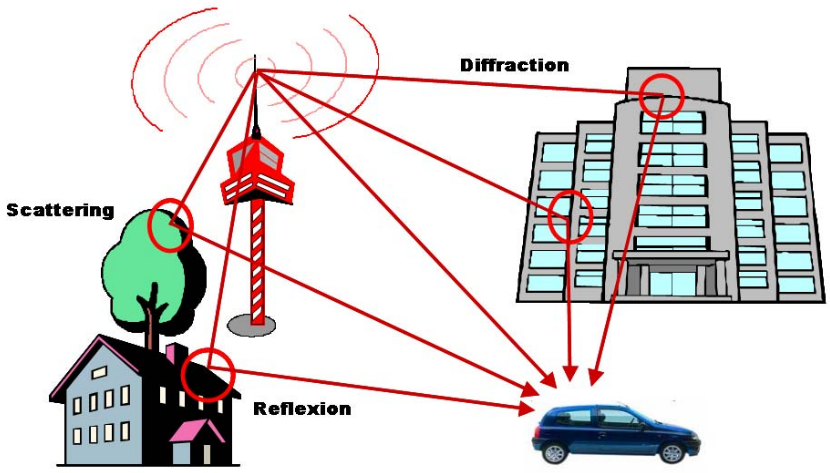

Figure 3.1: Phenomena involved in radio communication multipath

3.1.1 Phenomena involved in radio communication

The wave propagation in a homogeneous medium is described by the plane wave properties. The electromagnetic phenomena occurring at obstacles, as well as the speed of the receiver, impact the frequency, the phase and the strength of signal.

For a plane wave, the received signal can be written as the complex expression:

$$y(t) = A.e^{j(wt-\phi(t))} \tag{3.1}$$

or in baseband notation:

$$y(t) = A.e^{j\phi(t)} \tag{3.2}$$

where A is the signal amplitude also called envelope, w the angular frequency and $\phi(t)$ the signal phase.

Fading:

The environment of the receiver is not stationary; therefore, the phase of the received multipath component changes, affecting the received amplitude. The signal variation is often described according to two scales, the fast fading (microscopic fading) and slow fading (or macroscopic fading).

Doppler spread:

When the receiver is moving, the signal is subject to additional distortions in the frequency domain due to the receiver speed. Those distortions are called Doppler spread centered in the interval $[F_c - F_d, F_c + F_d]$ where F_c is the carrier frequency and F_d the maximum Doppler shift.

Delay spread:

The rays arriving at the receiver have followed different paths. Consequently, the propagation times also refer to delays and are related to the total distance the rays traveled. Those propagation time differences generate channel distortion called delay spread.

3.1.2 Fading

In the wireless context, destructive and constructive additions of multipath components leads to a gain difference at the receiver. Two scales of fading can be defined according to [2]:

Macroscopic fading

Macroscopic fading is caused by shadowing effects of buildings or natural features and determines the local mean of power. The statistical distribution of the local mean has been studied experimentally. The mean value of this distribution is influenced by the antenna heights, the operating frequency and the specific type of environment. However, it has been observed that the received power averaged over microscopic fading approaches a normal distribution when plotted on a logarithmic scale (i.e. in dB) and is called a log-normal distribution described by the probability density function (PDF)

$$f(w_{dB}) = \frac{1}{\sqrt{2\pi}\sigma} e^{-\frac{(w_{dB}-\mu)^2}{2\sigma^2}} \tag{3.3}$$

In the above equation w_{dB} (in decibel) is a random variable representing the long term signal power level fluctuation. μ and σ are respectively the mean and the standard deviation of w_{dB}. μ is equal to the distance dependent path loss.

Microscopic fading

Microscopic fading refers to the rapid fluctuation of the received signal in space, time and frequency, and is caused by the signal scattering off objects between the transmitter and receiver. If we assume that fading is caused by the superposition of a large number of independent scattered components, then the in-phase and quadrature components of the received signal can be assumed to be zero mean Gaussian processes. The envelope of the signal has a Rayleigh PDF given by:

$$f(x) = \frac{2x}{\omega} e^{\frac{x^2}{\omega}} u(x) \tag{3.4}$$

where ω is the average received power and u(x) is the unit step function defined as :

$$\begin{cases} u(x) = 1 & \text{if} \quad x \geq 0 \quad x \in \Re \\ u(x) = 0 & \text{if} \quad x < 0 \quad x \in \Re \end{cases} \tag{3.5}$$

If there is a direct (possibly LOS) path present between transmitter and receiver, the signal envelope is no longer Rayleigh and the distribution of the signal amplitude is Ricean. The Ricean distribution is often defined in terms of the Ricean factor, K, which is the ratio of the power in the mean component of the channel to the power in the scattered (varying) component. The Ricean PDF of the envelope of the received signal is given by:

$$f(x) = \frac{2x(K+1)}{\omega} e^{\frac{-K-((K+1)x^2)}{\omega}} I_0(x) 2x \sqrt{\frac{K(K+1)}{\omega}} u(x) \tag{3.6}$$

where ω is the mean received power as defined earlier and $I_0(x)$ is the zero order modified Bessel function of the first kind defined as :

$$I_0(x) = \int_0^{2\pi} e^{-xcos(\theta)} \, d\theta \tag{3.7}$$

In absence of direct path (K=0), the Ricean PDF reduces to the Rayleigh PDF since $I_0(x) = 1$. There exists more sophisticated fading distributions such as the Nagami distribution describing fading in high frequency channel.

3.1.3 Delay spread

In the multipath context, the arrival time of rays rely on the traveled distance of the electromagnetic wave. Usually, it is very complicated to identify the main component among all the multipath components. Let us consider an impulse equal to the symbol duration Ts. If the number of multipath components is high, the impulse response at the receiver side is constituted by a succession of impulses delayed and with different amplitudes. The original impulse has been spread over a time length that is expressed with σ_t and is illustrated in Figure 3.2.The delay spread is usually measured or estimated using the channel properties.

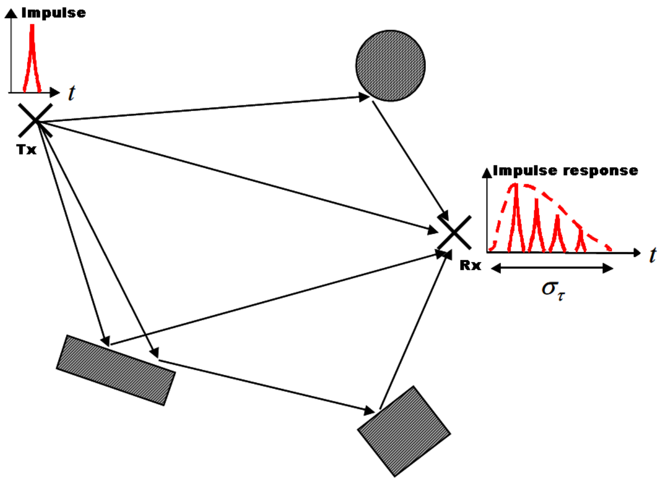

Figure 3.2: Pictorial representation of the delay spread

When the delay spread σ_t is negligible compared to the symbol time Ts, we can consider that all multipath contributions are almost reaching the receiver at the same moment, in the time slot allocated for the symbol. On the other hand, when the delay spread is higher, the received multipath components arrive during but also after the time slot limit and interfere with the next symbols. This spreading generates ISI which causes errors at the demodulation process. To attenuate this unwanted effect, pre and post processing techniques (discussed in Chapter 4) have been developed.

In Figure 3.2, we can see that the maximum delay spread is linked to the obstacles position. In most cases, the delay spread is small when environment obstacles are close to the receiver and high when obstacles are located far away. However, as explained before, those values have to be compared with the duration of the symbols.

3.1.4 Spectral analysis: coherence bandwidth

The influence of the delay spread can also be analyzed in frequency domain using the channel transfer function or the frequency response. The impulse response is linked to the frequency response by a Fourier transform. If the impulse response has a small delay spread compared to the symbol time, the transfer function is approximately constant over the coherence bandwidth of the considered system. The channel is then labeled frequency flat. Contrarily, if the transfer function contains nulls in the frequency range considered, the channel is frequency selective. The space between nulls is inversely proportional to the maximum delay spread, as stated in the following expression:

$$\Delta F_{zero} = \frac{1}{\sigma_t} \tag{3.8}$$

Figure 3.3 shows the frequency obtained respectively for a delay spread of $0.1s$ (distance approx. $30m$) and $1s$ (distance approx. $300m$) for 2 paths:

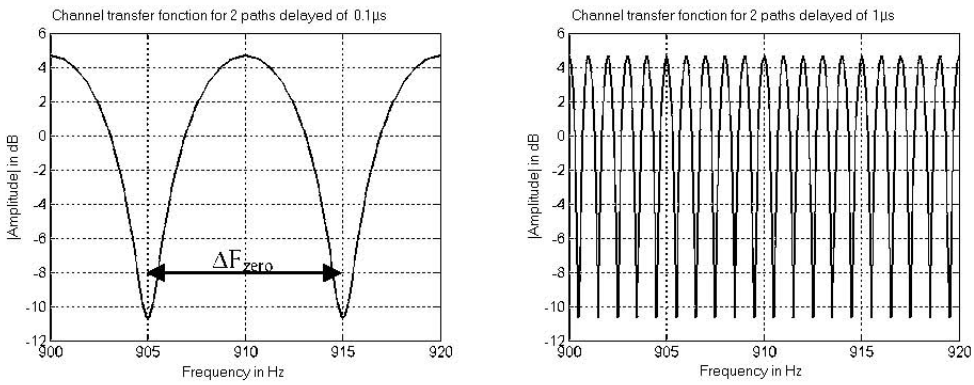

Figure 3.3: Channel response in frequency domain for 2 paths

The frequency range for which the transfer function is slowly varying is called the coherence bandwidth. All signal components in this range are affected in the same way by the propagation channel. The coherence bandwidth is usually defined according a frequency range where the correlation is lower than a certain value. There is not direct relation between the coherence bandwidth B_c and the delay spread. Nevertheless, those values are linked by a proportional relation:

$$B_c \propto \frac{1}{\sigma_t} \tag{3.9}$$

If $W = \frac{1}{Ts}$ is the band used by the considered signal, the channel is non-frequency selective when $B_c > W$.

3.2 Communication Systems

This section describes SISO and MIMO communication systems and channel models. In this section, lower case letter are used for functions in the time domain, whereas upper case letters are used for functions in the frequency domain. Vectors are written with an arrow, e.g. $\vec{x}$, and matrices with capital letters, e.g. $\mathbb{H}$.

3.2.1 SISO

The SISO communication system can be described as a time-variant linear system, associated to its transfer functions in either time or frequency domain.

We use two main functions to model the channel:

- The impulse response function $h(t, \tau)$
- The transfer function $H(f, t)$

t being the time, τ the delay (with respect to a certain t) and f the frequency.

Impulse response:

Concerning the impulse response [?], the input signal $x(t)$ and output signal $y(t)$ are linked by a convolution product:

$$y(t) = h(t, \tau) \otimes x(t) + n(t) \tag{3.10}$$

where $n(t)$ is the noise added at the receiver. This can also be written:

$$y(t) = \int_{-\infty}^{+\infty} h(t, \tau).x(t - \tau)\, d\tau + n(t) \tag{3.11}$$

A SISO communication system is represented on Figure 3.4.

The signal is sent from a transmitter (Tx) to a receiver (Rx). The impulse response of the channel describes the radio channel in the time domain. We can also express this function in a complex form (since we are dealing with baseband), introduced when the emitted symbols are represented by delayed impulses:

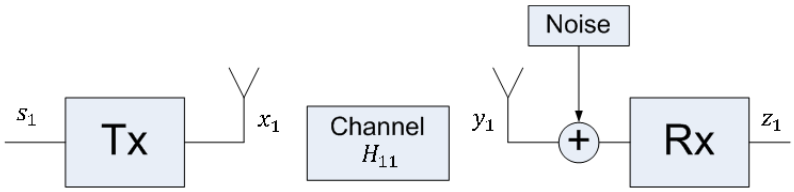

Figure 3.4: A SISO communication system

$$h(t,\tau) = \sum_{i=0}^{\infty} a_i(t) e^{j\phi_i(t)} \delta(\tau - \tau_i) \tag{3.12}$$

Where $a_i(t)$ is the amplitude associated to the delay τ_i and phase ϕ_i. Generally, this form is used for small-scale signal variations. In this case, the $a_i(t)$ or $a_i(t)e^{j\phi_i(t)}$ coefficients represent quick signal variations and follow a Rayleigh or Rice distribution, depending on whether there is a main path or not between Tx and Rx.

Transfer function:

Regarding the transfer function $H(f,t)$, the channel can also be described in the frequency domain through the time-variant frequency response. $H(f,t)$ corresponds to the channel response in frequency when excited at a moment t by a sinusoidal wave of frequency f. We can link h and H by the Fourier transform:

$$h(t,\tau) = \int_{-\infty}^{+\infty} H(f,t) e^{j2\pi f\tau} \, df \tag{3.13}$$

Let $Y(f)$ and $X(f)$ the Fourier transforms of, respectively, $y(t)$ and $x(t)$, the equation linking received and emitted signals in the frequency domain is:

$$Y(f) = H(f,t).X(f) + N(f) \tag{3.14}$$

In the temporal domain:

$$y(t) = \int_{-\infty}^{+\infty} Y(f).e^{j2\pi ft} \, df$$

3.2.2 MIMO

In this section is introduced the MIMO communication system and its associated equations. Then, some of the various MIMO techniques along with important notions are presented.

Introduction to MIMO

MIMO techniques introduce the use of multiple antennas at both ends of the communication system. An application is the combination of signals, at the transmitter or at the receiver, increasing the robustness of the link when the channel is undergoing multipath or suffering from interference. MIMO uses beam-forming and spatial diversity amongst other methods increasing effectiveness (in terms of SNR, capacity...) over a SISO link.

Based on a communication system using N_{Tx} antennas at the transmitter and N_{Rx} antennas at the receiver, the MIMO system can be seen in Figure 3.5.

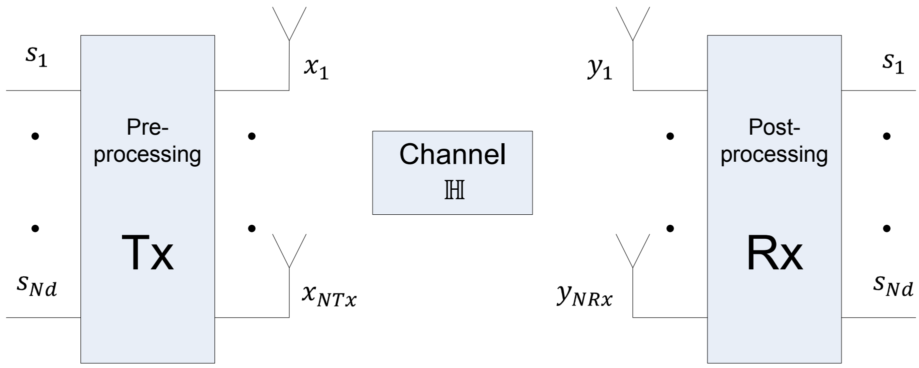

Figure 3.5: A MIMO communication system

The general expressions of the input and received signals along with the ones of the noise and the channel can be given in a matrix or vector form. Indeed, the signals $\vec{x}(t)$, $\vec{y}(t)$ and the noise $\vec{n}(t)$ are here vectors containing all the sent signals, received signals and noises. The channel $\mathbb{H}$ is a matrix containing all the links between each Tx and Rx, as:

$$\vec{y}(t) = \begin{bmatrix} y_1(t) \\ y_2(t) \\ \vdots \\ y_j(t) \\ \vdots \\ y_{N_{Rx}}(t) \end{bmatrix} \quad \mathbb{H} = \begin{bmatrix} h_{11} & \dots & h_{1j} & \dots & h_{1N_{Rx}} \\ & \ddots & & & \\ \vdots & & h_{ij} & & \vdots \\ & & & \ddots & \\ h_{N_{Tx}1} & \dots & h_{N_{Tx}j} & \dots & h_{N_{Tx}N_{Rx}} \end{bmatrix}$$
$$\vec{x}(t) = \begin{bmatrix} x_1(t) \\ x_2(t) \\ \vdots \\ x_i(t) \\ \vdots \\ x_{N_{Tx}}(t) \end{bmatrix} \qquad \vec{n}(t) = \begin{bmatrix} n_1(t) \\ n_2(t) \\ \vdots \\ n_j(t) \\ \vdots \\ n_{N_{Rx}}(t) \end{bmatrix} \tag{3.15}$$

where $x_i(t)$ is the sent signal at the ith antenna, $y_j(t)$ the received signal at the jth antenna. Equation 3.10 then becomes:

$$\vec{y}(t) = \mathbb{H}\vec{x}(t) + \vec{n}(t) \tag{3.16}$$

where $\mathbb{H}$ is the channel matrix of N_{Tx} x N_{Rx} dimensions, $\vec{x}$ the input signal, being the bit stream modulated (and then processed or not), and $\vec{n}$ the added noise.

In a medium presenting a lot of multipath, the use of various antennas at both the Tx and the Rx ends introduces several independent channels that correspond to propagation modes called Eigenmodes. The number of Eigenmodes corresponds to the rank of the channel matrix, complying to the constraint $rank(\mathbb{H}) \leq min(N_{Tx}, N_{Rx})$. MIMO allows a greater spectral efficiency than SISO thanks to the signal processing techniques used, jointly using temporal and spatial dimensions of the signal.

MIMO techniques

Different techniques are used depending on the objective (rate increase, robustness increase) but also on the information we have about the channel. When the channel is invariant during the processing time in both time and frequency, the techniques used concern coding schemes and adaptive modulation. Among them, we can mention:

- Spatial multiplexing
- Space-time coding

In addition, when the useful bandwidth of the signal becomes greater than the coherence bandwidth, the frequency selectivity of the channel introduces inter-symbol-interference (ISI). Depending on the knowledge of the channel, various techniques can be used. To name a few:

- MIMO techniques with CSI at the Tx (pre-processing):
  - Pre-filtering
  - Power allocation
  - Rate allocation
- MIMO techniques without CSI at the Tx:
  - Space-time block coding
  - Rate adjustment based on long-term average of SNR

These techniques introduce notions regarding diversity, array gain and multiplexing gain that we are going to explain.

Diversity

Diversity (and more precisely, Microdiversity) is one of the best techniques to mitigate the effects of multipath fading and improve energy efficiency. In a SIMO, MISO or MIMO communication system, it is very unlikely that independent signal paths experience the same deep fades simultaneously. The idea behind diversity is to send the same bits over these paths. Thus, we combine them in a way that the fading of the resultant signal is reduced.

Different types of diversity exist:

- Space diversity: uses multiple transmit or receive antennas where they are separated in distance.
- Frequency diversity: transmits the same Narrowband signal at different carrier frequencies, where the carriers are separated by the coherence bandwidth of the channel.

The performance advantage of a diversity system can be quantified. Indeed, the increase in SNR (due to diversity) leads to a decrease in error probability and the resulting advantage in data rate is called diversity gain. For MIMO systems, we talk about multiplexing gain, as there are multiple antennas at both the transmitter and the receiver. The average probability of symbol error for some diversity schemes can be expressed as [3]:

$$Ps_{avg} = c.SNR_{avg}{}^{-N_d} \tag{3.17}$$

where c is a constant that depends on the specific modulation and coding and N_d the diversity order of the system.

The diversity order tells how the slope of the average probability of error as a function of average SNR changes with diversity and can be derived from the number of antennas of the system:

$$N_d = N_{Tx}.N_{Rx} \tag{3.18}$$

Array gain

The array gain is defined as the increase in the SNR due to the coherent combining of the diversity signals. This can take place either in an AWGN channel or a channel suffering from fading. It is expressed:

$$A_g = \frac{SNR_{\Sigma avg}}{SNR_{avg}} \tag{3.19}$$

where $SNR_{\Sigma avg}$ is the average combined SNR and SNR_{avg} is the average SNR of a specific branch (that could be seen as a SISO link).

This allows a system with multiple transmit or receive antennas in a fading channel to achieve better performance than a system without diversity in an AWGN channel with the same average SNR.

3.3 Channel State Information and Estimation Errors

3.3.1 Channel State Information

Channel state information is the information about the current value of $\mathbb{H}$. At the receiver, the current value of $\mathbb{H}$ is necessary, in general to recover the transmitted data. At the transmitter, the knowledge of the channel can improve drastically the performance. This knowledge can be: the current value of channel, the mean value (long term average), the covariance, the distribution and so on. This type of information is generally referred as CSI and is usually estimated. Besides, the current value of $\mathbb{H}$ is referred to as short-term CSI, while the high order statistics of $\mathbb{H}$ are referred to as long-term CSI.

3.3.2 Channel estimation

The estimation of the CSI of a channel is sorely perfect. However, CSI at the Rx is easier to estimate than at the Tx because the Rx can perform quasi-instantaneous estimation based on signals received. On the contrary, the Tx needs the information to be fed back to it. The feedback introduces the problem of delay. Indeed, it is performed periodically, so the information of the channel may not fit anymore when it is used.
The TDD system uses, in general, the reciprocity properties of the channel, which means it assumes the channel from the transmitter to the receiver is approximately the same as the channel from the receiver to the transmitter. This assumption allows to avoid the use of feedback mechanism.

Estimation techniques

Different approaches are commonly used to estimate a channel :
- Training based
- Blind
- Semi-blind
- Hidden pilot

In the training-based approach, a sequence known to the receiver is transmitted in the acquisition mode.
In blind approaches, no such sequence is available (or used) and the channel is estimated based solely on the noisy received signal exploiting the statistical

and other properties of the information sequence.
Semiblind approaches utilize a combination of training-based and blind approaches.
In the hidden pilot-based approaches, a periodic (non random) training sequence is arithmetically added (superimposed) at a low power to the information sequence at the transmitter before modulation and transmission.

Our project is restricted to the training based approach.

Two kinds of channel state estimations are commonly used:

- Channel statistics:
  This estimation begins with the description of the channel on a large time scale. Here, we predict the most probable behavior.

- Channel instantaneous:
  This method describes the channel instantaneous state. Here, we take into account the short scale fading.

Most of actual commercial systems are often based on channel statistics. Using the information of instantaneous channel require an higher computation load due to the swiftness of parameters values.

The Feedback mechanism

In order to understand how the feedback mechanism, used to acquire the channel at the Tx, introduces error in the estimation, let us consider a classical communication system.
The Base Station (Tx) transmits a training sequence from each antenna. This enables the Mobile Station (Rx) to recover all separate impulse responses. It then usually feeds the information back to the Base Station on a separate feedback channel.

The Channel instantaneous feedback has drawbacks:

- We have to make sure that the feedback occurs within a time that is less than the coherence time of the channel.

- The feedback channel decreases the spectral efficiency of the system. Indeed, this information is not user data. The performance of the system gets better with more feedback but a good compromise has to be found between the feedback resources used and total performance.

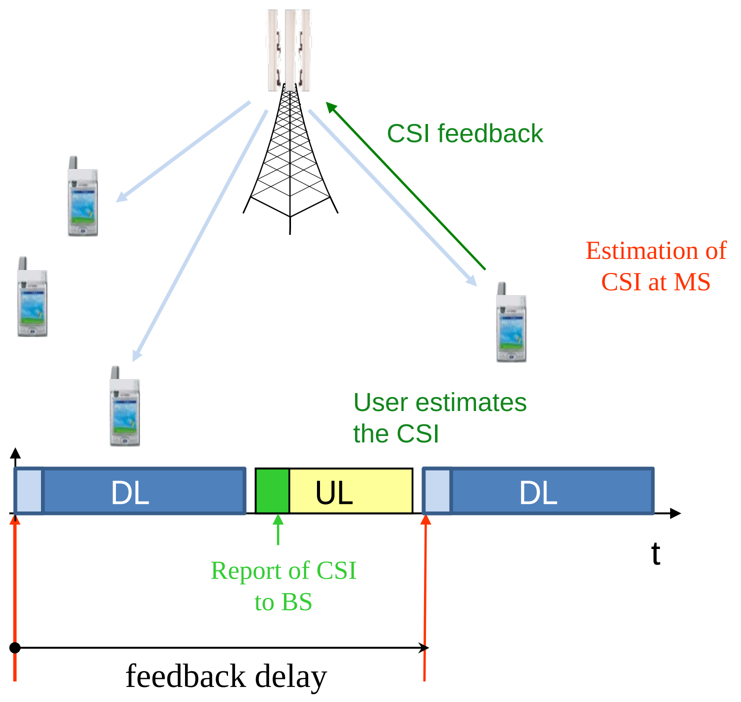

Figure 3.6: Outdated CSI in feedback context

Wireless channels are usually time variant. Feedback implies that the information received describes an anterior state which might no longer be realistic. Then, the CSI used to pre-process our signals are intrinsically outdated. The feedback mechanism is obviously one of the error sources in the estimation of the channel. The errors depend on how fast the channel changes.

Chapter 4

Eigenmode-based pre-processing schemes

4.1 Eigenmode Transmission

Eigenmode transmissions define mathematically the channel properties (strength of links); Eigenmodes are commonly used to perform post or pre-processing in MIMO situation. They are extracted by a mathematical method named Singular Value Decomposition (SVD).

Given the linear transformation $\mathbb{A}\vec{x} = y$, the non-zero vector $\vec{x}$ is defined as an eigenvector of this transformation if it satisfies the eigenvalues equation

$$\mathbb{A}\vec{x} = \lambda\vec{x}$$

where λ is a scalar defined as an eigenvalue associated to the eigenvector $\vec{x}$.

SVD is a technique usually used in wireless communication to extract information from a channel. A channel matrix noted H can be decomposed into a product of 3 matrices as follows:

$$\mathbb{H} = \mathbb{U}\Lambda\mathbb{V}^H \tag{4.1}$$

$\mathbb{U}$ and $\mathbb{V}$ are complex unitary matrices with sizes N_{Tx} x N_{Tx} and N_{Rx} x N_{Rx}, respectively. Λ is a N_{Tx} x N_{Rx} matrix which elements are zeros except for its main diagonal, which contains $min(N_{Tx}, N_{Rx})$ real non-negative singular values.

Figure 4.1 represents the MIMO communication system used for the Eigenmode transmission technique.

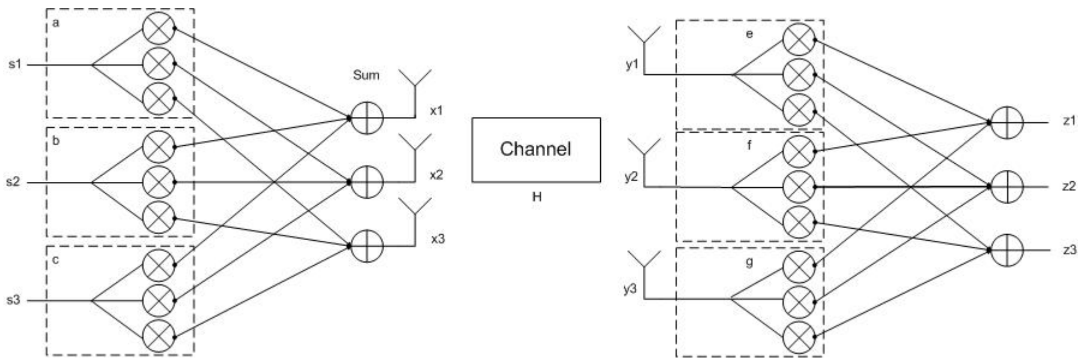

Figure 4.1: MIMO Eigenmode transmission system

In this case, we have 3 different signals, s_1, s_2, s_3, sent by 3 transmitters to 3 receivers. Each signal is multiplexed and sent to all 3 receivers. In order to demultiplex the signals at the receiver end, we introduce weights a_n, b_n, c_n ($n = 1, 2, 3$ the signal's number), respectively the ones processing the first signal, the second signal and the third signal.

The signals sent can then be expressed:

$$\begin{cases} x_1 = a_1 s_1 + b_1 s_2 + c_1 s_3 \\ x_2 = a_2 s_1 + b_2 s_2 + c_2 s_3 \\ x_3 = a_3 s_1 + b_3 s_2 + c_3 s_3 \end{cases} \tag{4.2}$$

These equations can be put in a matrix form. Thus,

$$\begin{bmatrix} x_1 \\ x_2 \\ x_3 \end{bmatrix} = \begin{bmatrix} a_1 & b_1 & c_1 \\ a_2 & b_2 & c_2 \\ a_3 & b_3 & c_3 \end{bmatrix} \times \begin{bmatrix} s_1 \\ s_2 \\ s_3 \end{bmatrix} \tag{4.3}$$

Let the transmitted weight matrix be $\mathbb{W}$, equation 4.3 becomes:

$$\vec{x} = \mathbb{W}\vec{s} \tag{4.4}$$

Now we have introduced weights for each signal, let us write the vector of signals sent through the channel:

$$\vec{y} = \mathbb{H}\vec{x} + \vec{n} \tag{4.5}$$

Using equation 4.1, this becomes:

$$\vec{y} = \mathbb{U}\Lambda\mathbb{V}^H\mathbb{W}\vec{s} + \vec{n} \tag{4.6}$$

Let $\mathbb{W} = \mathbb{V}$. This way, $\mathbb{V}^H\mathbb{W} = \mathbb{I}$, and 4.6 becomes:

$$\vec{y} = \mathbb{U}\Lambda\vec{s} + \vec{n} \tag{4.7}$$

On the receiver end, we receive the signals contained in $\vec{Y}$, i.e. y_1, y_2, y_3 that we demultiplex with weights e_n, f_n, g_n to recover the signals z_1, z_2, z_3.

Combined with weights, the received signals can then be expressed:

$$\begin{cases} z_1 = e_1 y_1 + f_1 y_2 + g_1 y_3 \\ z_2 = e_2 y_1 + f_2 y_2 + g_2 y_3 \\ z_3 = e_3 y_1 + f_3 y_2 + g_3 y_3 \end{cases} \tag{4.8}$$

These equations can be put in a matrix form. Thus,

$$\begin{bmatrix} z_1 \\ z_2 \\ z_3 \end{bmatrix} = \begin{bmatrix} e_1 & f_1 & g_1 \\ e_2 & f_2 & g_2 \\ e_3 & f_3 & g_3 \end{bmatrix} \times \begin{bmatrix} y_1 \\ y_2 \\ y_3 \end{bmatrix} \tag{4.9}$$

Let the received weights matrix be $\mathbb{J}$, equation 4.9 becomes:

$$\vec{z} = \mathbb{J}\vec{y} \tag{4.10}$$

Using 4.6, equation 4.10 becomes:

$$\vec{z} = \mathbb{J}\mathbb{U}\Lambda\vec{s} + \mathbb{J}\vec{n} \tag{4.11}$$

Let $\mathbb{J} = \mathbb{U}^H$, 4.11 becomes:

$$\vec{z} = \Lambda\vec{s} + \mathbb{U}^H\vec{n} \tag{4.12}$$

In a matrix form:

$$\vec{z} = \begin{bmatrix} \lambda_1 & 0 & 0 \\ 0 & \lambda_2 & 0 \\ 0 & 0 & \lambda_3 \end{bmatrix} \times \begin{bmatrix} s_1 \\ s_2 \\ s_3 \end{bmatrix} + \vec{\tilde{n}} \tag{4.13}$$

We simplify this expression:

$$\vec{z} = \begin{bmatrix} \lambda_1 s_1 + \tilde{n}_1 \\ \lambda_2 s_2 + \tilde{n}_2 \\ \lambda_3 s_3 + \tilde{n}_3 \end{bmatrix} \tag{4.14}$$

We notice here that only the components of each transmitted signal are present in each received signal. There is no inter-stream interference. This is due to the use of weights that guarantees the reception of only the desired signal at the receiver end.

Moreover, if we are using the power allocation algorithm (Water-filling) discussed in Section 4.3, we can reallocate the powers among the remaining streams (complying with the BER threshold constraint stated in Section 4.2 on Table 4.1). Also, now we have obtained Λ, we can determine the post-processing SNR, as:

$$SNR_i = \frac{\lambda_k^2 P_k}{\sigma_n^2} \tag{4.15}$$

λ_k and P_k being the eigenvalue and power of the kth link and σ_n^2 the noise variance.

Once the post-processing is performed, the expression of the signal can be written as on equation 4.16 with:

$$z_n(t) = P_k \lambda_k s_n(t) + n_n(t) \tag{4.16}$$

where $z_n(t)$, $s_n(t)$ and $n_n(t)$ are related to the nth signal.

4.2 Adaptive Modulation and Coding

The concept of AMC is to adjust the modulation and the coding to the channel characteristics (e.g. path loss, interference... see section 3.1) in order to improve performance (rate of transmission, BER, spectrum efficiency...). There are many parameters on which the adaptation can be performed, such as data rate, power, coding, error probability. In our case, we only adjusted the modulation with respect to a certain BER threshold. These systems require some channel information at the transmitter that can be obtained through the methods stated in Section 3.3.

The matching of the modulation to the most appropriate one occurs throughout the whole transmission. The first step is to sketch a range of SNRs that will help us identify the levels of modulation. From a SISO AWGN channel, we draw the curves of the BER with respect to the SNR. The BER threshold will determine the SNRs levels at which a higher modulation is more appropriate to transmit the signal. The goal here is to keep the BER under the target level (threshold) and maximize the throughput by increasing the order of modulation used to send the signal. Figure 4.2 displays those ranges:

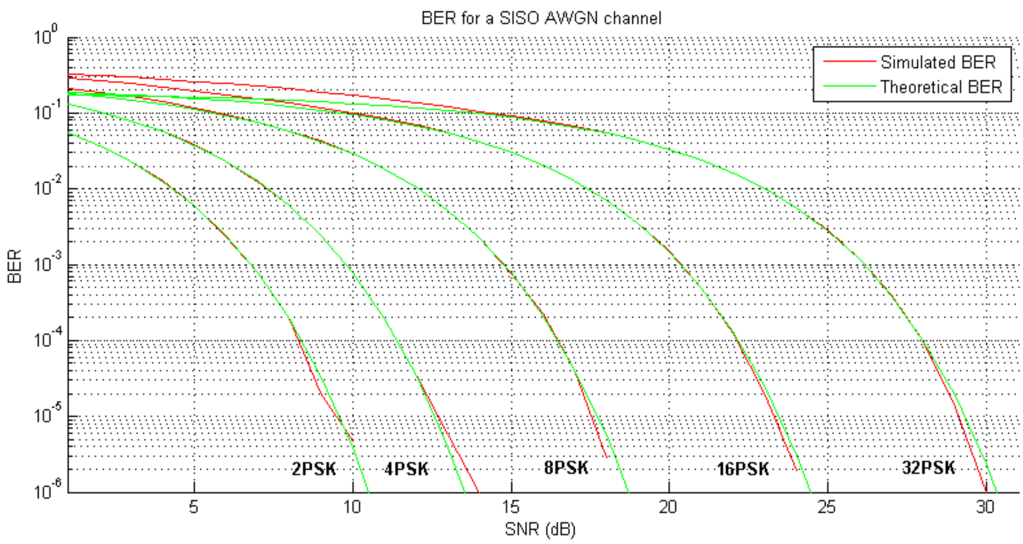

Figure 4.2: BER versus SNR curves for a SISO AWGN channel

We have decided to set the BER threshold at 10^{-2}, therefore, the ranges will be as in Table 4.1:

SNR range(dB)	Under 4.3	4.3 to 7.3	7.3 to 12	12 to 17.4
Modulation	No signal	BPSK	QPSK	8PSK
SNR range(dB)	17.4 to 23	23 to 28.6	28.6 and above	
Modulation	16PSK	32PSK	64PSK	

Table 4.1: Modulation used for AMC with respect to the SNR range for a BER threshold of 10^{-2}

There is a difference between the theoretical and simulated BER. The theoretical BER is an approximation which is not accurate for low SNR and high order modulations.

Moreover, the values of the BER for a SNR below 4.3 dB are higher than 10^{-2}. This does not comply with the threshold we have set and therefore, in this case, we decide not to send any signal. Even though the total throughput will be substantially lower (0 until 4.3 dB), the BER is above the threshold set.

Once the AMC thresholds are determined, we calculate the instantaneous post-processing SNR at the receiver with equation 4.15.

We then compare these instantaneous SNRs with the previously obtained AMC thresholds. This way, the best modulation order needed to transmit the signal during this realization is known. If there is no transmission over one or several streams ($SNR_{inst} < 4.3dB$) and we are using the power-allocation algorithm named Water-filling (discussed in section 4.3), we re-allocate the powers between the remaining streams. We then need to re-calculate the instantaneous SNRs (as the number of transmitting streams has changed). From those new SNR_{inst} comes a new adaptation of the modulation. This process is repeated until all the streams have a $SNR_{inst} > 4.3dB$.

The goal here is to always remain under the BER threshold while maximizing the throughput.

As we mentioned before, AMC can be coupled with a Power-Allocation technique, such as Water-filling to increase all the more the performance, as the available power will be divided proportionally amongst the best links in a descending order. We are going to discuss this in the following section.

4.3 Water-filling

4.3.1 Main concept

The goal of the Water-filling is to allocate the power over the streams to maximize the capacity. Using the SVD to decompose the channel we can express the channel $\mathbb{H}$ as :

$$\mathbb{H} = \mathbb{U}\Lambda\mathbb{V}^H \tag{4.17}$$

The Λ matrix contains the singular values which are used to express the attenuations of the sub channels. The channel will be power filled according to those attenuations. The sum of all sub channels power has to be less than a given total power :

$$\sum_{k=1}^{n} P_k \leq P_t \tag{4.18}$$

P_t is the total power, P_k is the power of the kth sub channel.

In our case, we assume:

$$\sum_{k=1}^{n} P_k = P_t \tag{4.19}$$

The problem is to find the power allocation that maximize the capacity under the transmit power constraint. Using the capacity formula, assuming each stream is independent and consequently that the maximum throughput of the system is equivalent to the sum of the throughput of each stream, the problem could be written as :

$$\max \sum_{k=1}^{n} log_2 \left(1 + \frac{\lambda_k^2 P_k}{\sigma_n^2}\right) \tag{4.20}$$

where λ_k^2 is the attenuation for the kth sub channel and σ_n^2 the noise variance. This optimization problem is solved using the Lagrange multiplier which gives us an equivalent:

$$\max_{P_k, v} \sum_{k=1}^{n} log_2 \left(1 + \frac{\lambda_k^2 P_k}{\sigma_n^2}\right) - v(\sum_{k=1}^{n} P_k - P_t\Big) \tag{4.21}$$

taking the derivative with respect to P_k, we obtain:

$$P_k = (\frac{1}{v} - \frac{\sigma_n^2}{\lambda_n^2}\Big)^+ \quad (4.22)$$

where $(.)^+$ means $P_k > 0$. $P_k = 0$ for negative values.

4.3.2 Graphical representation

This formula allows us to find the waterline, and fill each sub channel. A common graphical representation of water-filling can be seen on figure 4.3 :

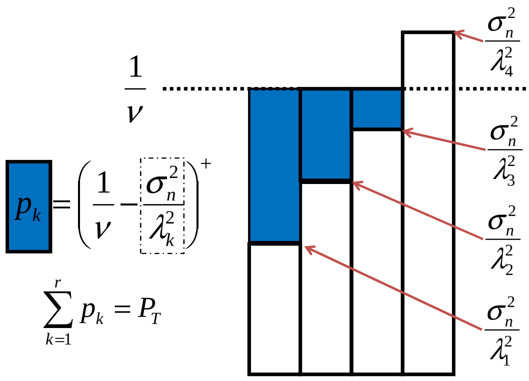

Figure 4.3: Water-filling pictorially

This is an example of a transmission of 4 streams, the 4^{th} one not receiving any power because the ratio $\frac{\sigma_n^2}{\lambda_4^2}$ is over the waterline $\frac{1}{v}$.

4.3.3 AMC and Water-filling

In order to stay below the AMC BER threshold, the AMC technique prevents the transmission of some streams. Indeed, a too low instantaneous SNR will lead to an undesirable BER. When some streams are removed, the Water-filling technique is impacted. It may happen that some power has been allocated to a stream which is doomed to disappear. A new pass of Water-filling is required to spread the power over the remaining streams. The process can be seen of Figure 4.4.

When an additional pass is required, a new waterline is defined.

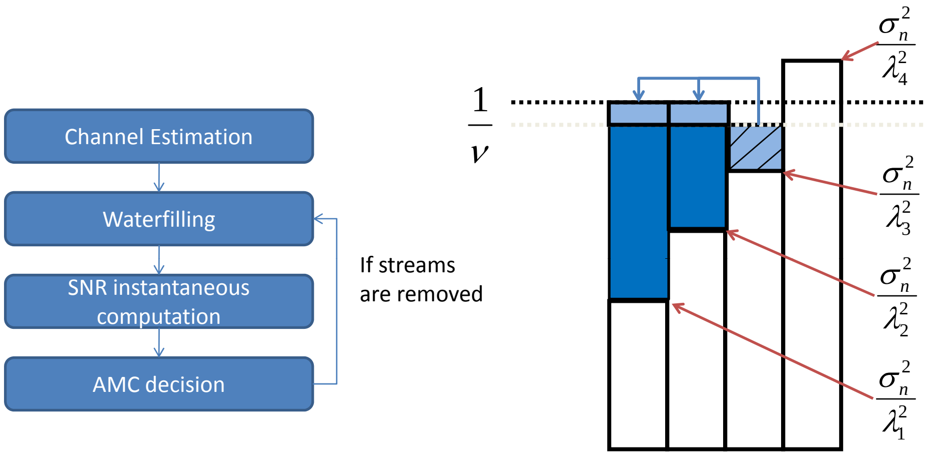

Figure 4.4: Water-filling pictorially

Chapter 5

CSI estimation errors and Modeling

In order to use processing techniques, CSI is needed. In general, the CSI cannot be perfectly acquired at the transmitter. We can distinguish two main type of estimation error for continuous fading channels :

- Error due to noise in the estimation process
- Error due to the temporal changes in the channel, which rely on Doppler.

5.1 Estimation with noise errors

The estimated channel $\hat{\mathbb{H}}$, taking into account only noise error, can be described as :

$$\hat{\mathbb{H}}_{no} = \mathbb{H} + \sigma_{\mathbb{H}_{error}}\mathbb{N} \tag{5.1}$$

where $\mathbb{N}$ is a matrix of dimensions N_{Tx} x N_{Rx} with zero-mean circularly symmetric complex Gaussian (ZMCSCG) entries with a variance of 1.
$\sigma_{\mathbb{H}_{error}}$ is the standard deviation of the CSI error.

The simplest method to represent the noise due to errors is the following: The error between the channel $\mathbb{H}$ and the estimation containing error $\hat{\mathbb{H}}$ will be proportional to the mean value of $\mathbb{H}$, so we can set a given value of error SNR :

$$SNR_{\mathbb{H}_{est}} = \frac{E[|\mathbb{H}^2|]}{E[|(\hat{\mathbb{H}} - \mathbb{H})^2|]} = \frac{1}{\sigma^2_{\mathbb{H}_{error}}} \tag{5.2}$$

A more advanced representation is to use the training based approach which is widely used in TDD systems. The error is related to the quality of the estimation directly influenced by the length of the training sequence :

$$SNR_{\mathbb{H}_{est}} = SNR_i + T = \frac{1}{\sigma^2_{\mathbb{H}_{error}}} \tag{5.3}$$

where $SNR_i(dB)$ is the average channel SNR.
$T(dB)$ is the quality of the estimation related to the length of the training sequence :

$$10^{\frac{T}{10}} \propto \frac{1}{L} \tag{5.4}$$

where L is the length of the training sequence.
$T = inf$ means perfect estimation, with an infinite training sequence.

5.2 Estimation with Doppler errors

A simplified representation of the error induced by the Doppler effect can be made using the parameter ρ which is the coefficient of correlation between $\hat{\mathbb{H}}$ and $\mathbb{H}$.

$$\hat{\mathbb{H}}_{do} = \rho\mathbb{H} + \sqrt{1-\rho^2}\mathbb{N} \tag{5.5}$$

The correlation coefficient decreases as the feedback delays increases.

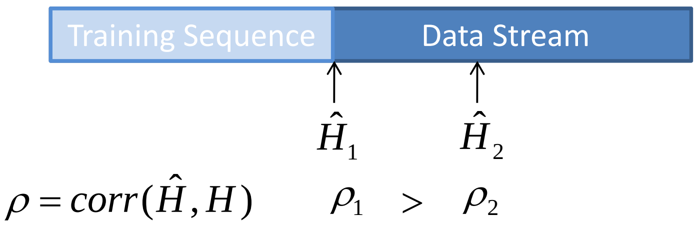

Figure 5.1: Example of a training sequence

The correlation coefficient describes how the channel has changed between two time samples. The correlation is linked to the speed of the receiver, which can be described in terms of Doppler frequency. The correlation coefficient ρ is linked to the maximum Doppler frequency f_{dmax} and to the delay τ between the two samples. If angles of arrival are uniformly distributed, the correlation can be written using the Bessel function J_o :

$$\rho(\tau) = J_o(2\pi f_{dmax}\tau) \tag{5.6}$$

Knowing that the maximum Doppler frequency can be express as:

$$f_{dmax} = f_c \frac{u}{c} \tag{5.7}$$

where f_c is the carrier frequency, u the receiver speed and c the speed of light.

Then, the correlation can be expressed in function of the distance traveled δ_l between two measures:

$$\rho(\tau) = J_o(2\pi f_{dmax}\tau) = J_o\left(2\pi\frac{f_c}{c}u\tau\right) = J_o\left(2\pi\frac{u\tau}{\lambda}\right) \tag{5.8}$$

$$\rho(\delta_l) = J_o\left(2\pi\frac{\delta_l}{\lambda}\right) \tag{5.9}$$

For example at 3Ghz and at 5Ghz, for a correlation of 0.9 according to the curves 5.2 and to the formula 5.9, the distance traveled by the receiver in movement is respectively 1.76 cm and 1.05 cm.

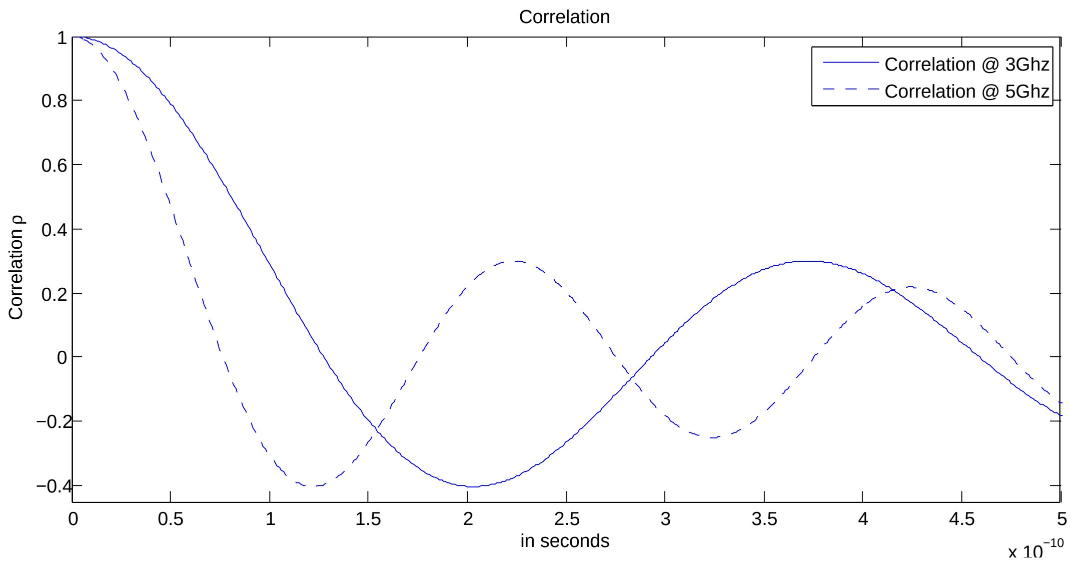

Figure 5.2: Correlation @ 3Ghz and 5Ghz

Chapter 6

Simulations

The aim of this project is to study the influence of CSI imperfections on Eigenmode-based pre-processing schemes. To do so, we conceived a simulator of various system configurations allowing us, according to the parameters of the simulation, to see how the presence of errors in the channel estimation is detrimental to the pre-processing techniques used at the transmitter. The project contributions are the simulations of the system performance. To model the channels and run the simulations, we used the software Matlab. We started from scratch and no outer sources were used to complete our simulations.

This chapter is divided into three parts.

First, we will go through the simulations run for a SISO communication system without CSI errors in section 6.1. Secondly, in section 6.2, we will analyze the results for a MIMO communications system with perfect CSI. And lastly, the case of a MIMO communications system with imperfect CSI will be discussed and the results commented in section 6.3.

6.1 SISO with perfect CSI

In this section, we will discuss the performance of a perfect SISO communication system (no CSI errors). Some of the code used for the simulations will be presented and commented, including channel modeling, BER calculation and result interpretation.

This section comprises two parts. First, we will discuss the Additive White Gaussian Noise (AWGN) channel model, and secondly, the Rayleigh fading model.

6.1.1 SISO AWGN channel

The SISO AWGN channel model is the simplest configuration we have simulated. It is also the one we have used to determine the SNR ranges that will be used for the AMC (see section 4.2). The channel model is the one mentioned in section 3.2.1 in figure 3.4. The block diagram of our code for a SISO AWGN channel can be seen on Diagram 6.1.

Equation 6.1 corresponds to equation 3.10 for a PSK transmission through a SISO AWGN channel:

$$y(t) = h.x(t) + n(t) \tag{6.1}$$

The channel is time-invariant and therefore is not a function of time. The SNR is determined according to equation 6.2.

$$SNR = \frac{P.E[|H|]^2}{\sigma_n^2} \tag{6.2}$$

where P is the transmit power of the link, H is the expression of the channel and σ_n^2 the noise variance.

For each order of modulation, we make the SNR vary (from 1 to 40 dB) and we both calculate and simulate the BER. First, we determine the standard deviation of the noise σ_n from the value of the SNR with $\sigma_n = \frac{1}{\sqrt{SNR}}$. We generate the channel ($\mathbb{H} = 1$) and the noise that follows a Gaussian distribution of variance σ_n^2 and mean zero. We then modulate the bit stream, send it through the channel (as in equation 4.5) and demodulate the signal received. From the number of errors between the transmitted and received bit streams, we determine the bit error probability.

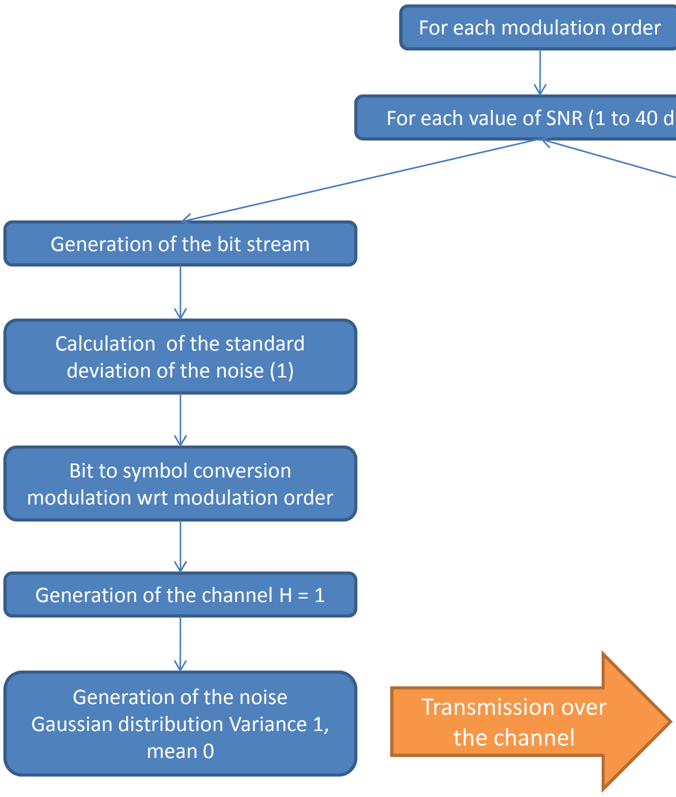

Figure 6.1: Block diagram for a SISO AWGN channel

For BPSK and QPSK, the following equation is used [4]:

$$P_b = Q\left(\sqrt{2\frac{\epsilon_b}{N_0}}\right) \tag{6.3}$$

where $N_0 \approx \sigma_n^2$ and $\frac{\epsilon_b}{N_0}$ is the Energy per bit to noise power spectral density ratio, a normalized version of the SNR, also known as SNR per bit.

However, for QPSK, the symbol error probability differs:

$$P_M = 2Q\sqrt{2\frac{\epsilon_b}{N_0}}\left(1 - \frac{1}{2}Q\sqrt{2\frac{\epsilon_b}{N_0}}\right) \tag{6.4}$$

Higher orders of PSK modulation introduce a symbol error probability that can be calculated as follows:

$$P_M = 2Q\sqrt{2k\frac{\epsilon_b}{N_0}}\left(\sin\frac{\pi}{M}\right) \tag{6.5}$$

where k is the modulation order, or number of bits per symbol ($k = \log_2(M)$) and M the constellation size.

This is an approximation that works best for high values of SNR which is the area we are interested in.

It is not always easy to find the equivalent bit error probability, since it depends on the mapping of k-bit symbols into the corresponding signal phases. However, when we use Gray code, two k-bit symbols corresponding to adjacent signal phases differ in only a single bit. Since the most probable errors due to noise result in the erroneous selection of an adjacent phase to the true phase, most k-bit symbol errors contain only a single-bit error. Hence, the bit error probability can be approximated as (for M-ary PSK modulation) [4]:

$$P_b \approx \frac{1}{k} P_M \tag{6.6}$$

Both the theoretical and simulated BER can be calculated, and compared. From theory, the BER as a function of the SNR is determined by the probability of error for each bit, as:

$$BER(SNR)_{theo} = P_b \tag{6.7}$$

From the simulations, we compare the received bit stream with the transmitted one and calculate how many errors occurred. Then, we divide this number by the total number of bits sent, again, for each value of the SNR:

$$BER(SNR)_{sim} = \frac{\sum(Errors)}{N_{bits}} \tag{6.8}$$

where $\sum(Errors)$ is the number of wrongly received bits and N_{bits} the total number of sent bits.

Plotting the BER with respect to the SNR, we obtain Figure 6.2:

We notice that the simulated BER fits almost perfectly with the theoretical one, except for low SNR at high order of modulation where the approximation used in the theoretical formula becomes inaccurate.

To have a better understanding of the influence of the modulation on the transmission, we have plotted both the probability of correctly receiving a symbol and the bit throughput curves per symbol time with respect to the SNR. Here, the time reference is the symbol time (presented in Section A.1)

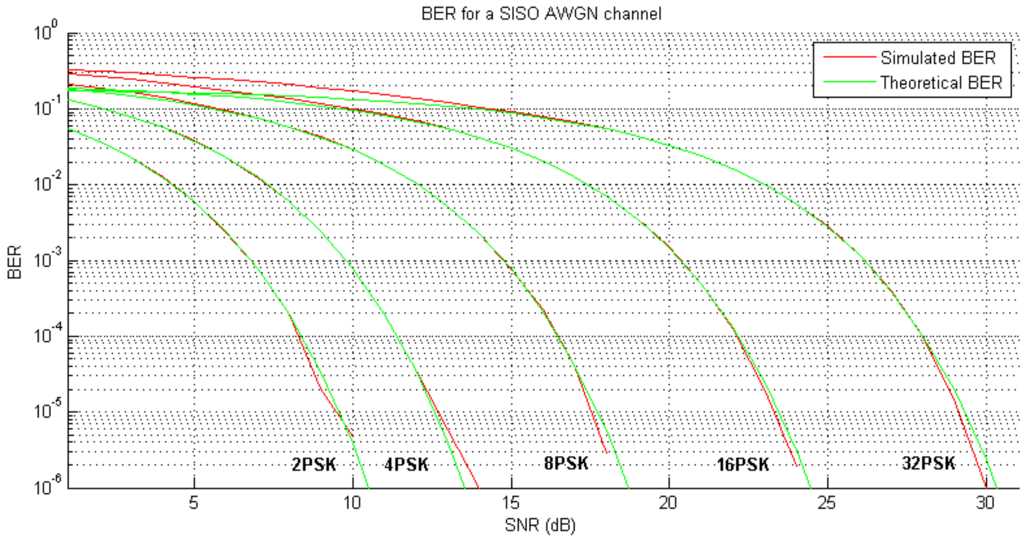

Figure 6.2: BER versus SNR for a SISO AWGN channel

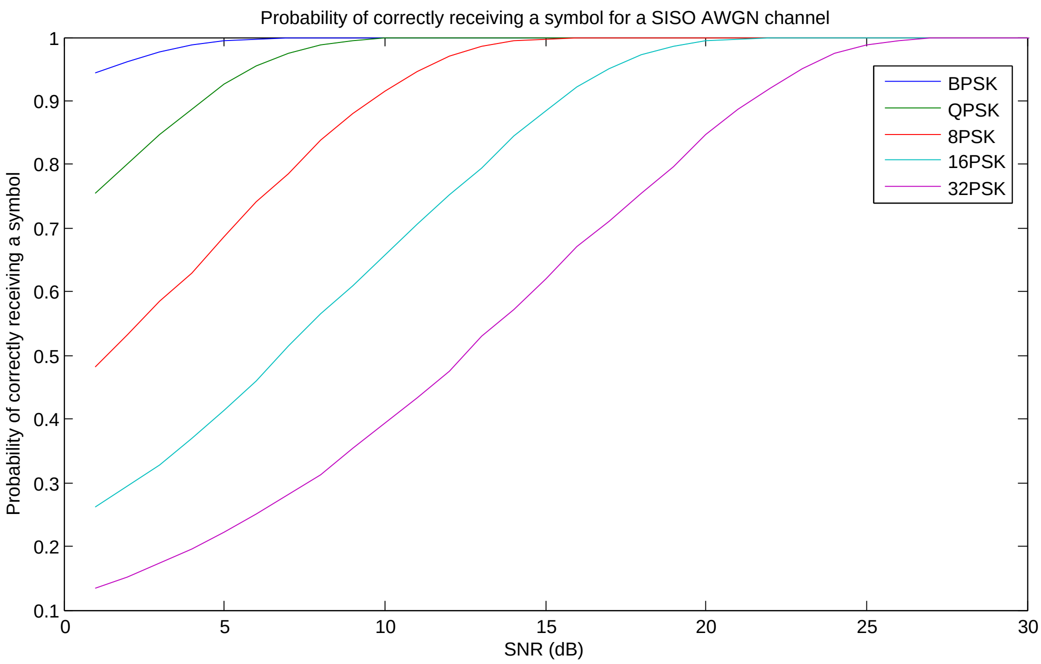

Figure 6.3: Probability of correctly receiving a symbol for a SISO AWGN channel

and only one transmission takes place at a time (SISO). The symbol probability can be seen in Figure 6.3:

We notice that for low modulation orders (BPSK and QPSK), the symbol sent is well received with low values of SNR. The throughput, however, remains low. With higher modulation orders, the number of symbols correctly received in only one Ts increases significantly.

For each SNR, we compute the throughput using Equation 6.9:

$$Throughput(SNR) = \frac{N_{bits} - \sum(Errors)}{N_{bits}} \tag{6.9}$$

Figure 6.4 displays the curves of the bit throughput for the same situation.

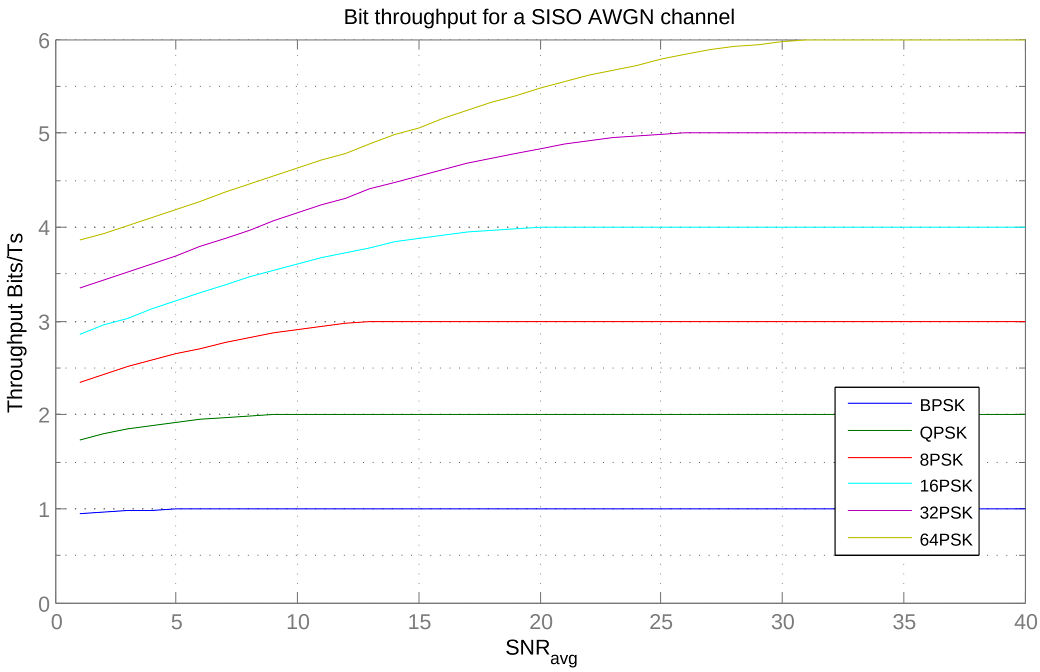

Figure 6.4: Bit throughput for a SISO AWGN channel

These curves allow us to see the correspondence between modulation orders and sent/correctly received data. From the first graph, the best case in which the least errors were encountered was certainly the BPSK. However, when it comes to rate of transmission, we notice that there are much better compromises between BER and throughput.

6.1.2 SISO Rayleigh Fading channel

Now, we are going to discuss the case where the channel suffers from Rayleigh fading. The difference between the preceding channel model and this one lies in the creation of the channel. Here, it is no longer constant but instead, is randomly generated and therefore introduces the phenomena mentioned in section 3.1.1, such as fading. The block diagram of our code for a SISO Rayleigh channel is presented on Diagram 6.5.

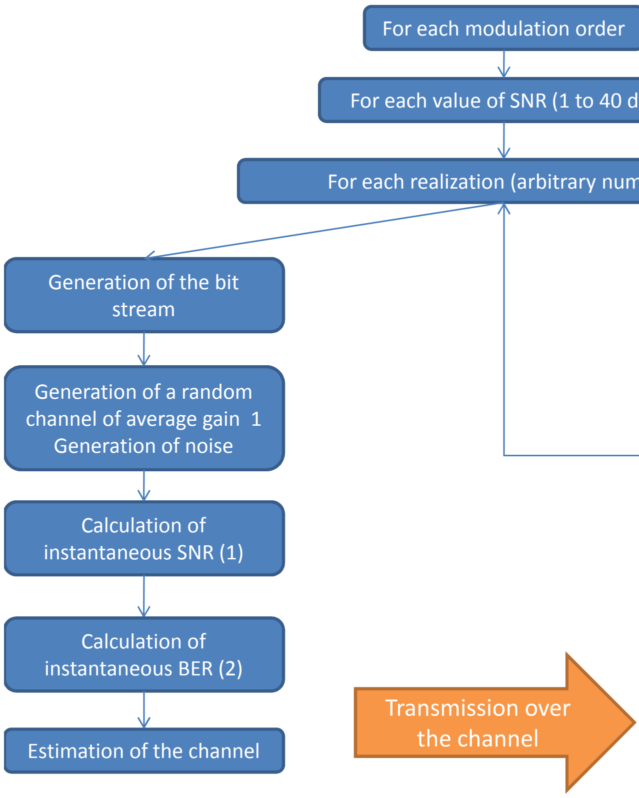

Figure 6.5: Block diagram for a SISO Rayleigh channel

Therefore, we rely on the instantaneous SNR to determine the BER (both simulated and theoretical). For each realization of the channel, and we obtain a different value of SNR_i with the same equation as for a SISO AWGN link, only here the channel varies:

$$SNR_i = \frac{P_t.\, E[|H|^2]}{\sigma_n^2} \tag{6.10}$$

Matlab offers many useful functions that we have been using throughout the simulations. One of these functions named *berfading* can plot the BER for a certain modulation type, constellation size, diversity and symbol mapping. This helped us checking our curves in addition to the formula introduced earlier and the simulated results. Figure 6.6 shows the curves of theoretical and simulated BER obtained with values of SNR_i along with the curve of BER obtained from Matlab's function *berfading* with respect to SNR.

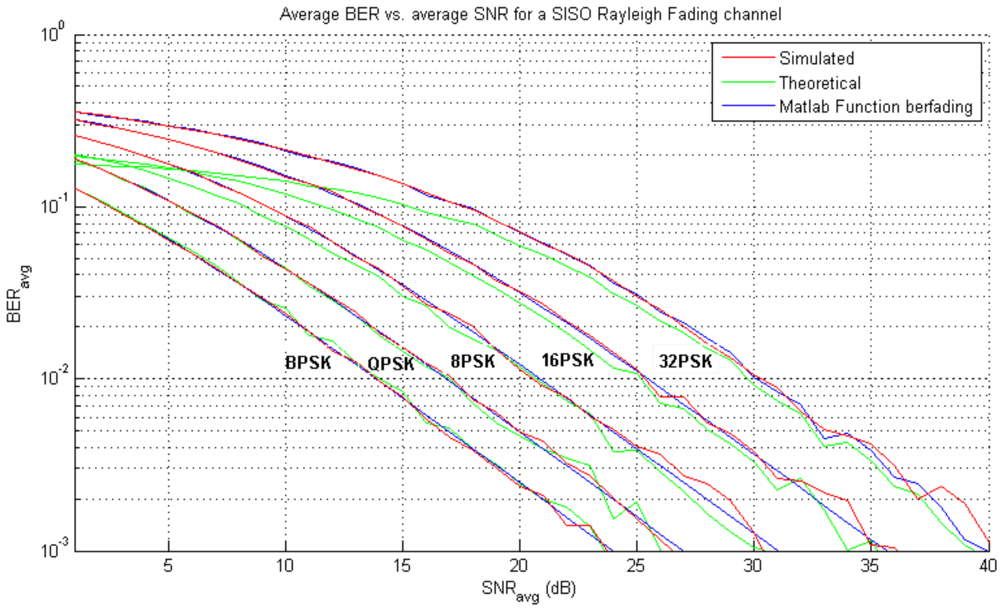

Figure 6.6: Average BER versus average SNR for a SISO Rayleigh channel

We notice, first, that the simulated curves correspond to the theoretical one perfectly. The variations we notice at high SNRs (from 25 to 40 using BPSK/QPSK) are explained by the number of realizations of the channel used to plot these curves. It requires a lot of realizations to get a smooth curve but it also substantially increases the computational complexity. This is due to the number of bits we send through the channel. Basically, the BER is based on the probability that a bit is wrongly received. If we do not have enough samples (bits) to base the calculation (or simulation) of the BER on, we will not have accurate values when it comes to very low probability (lower than 10^{-4}). We have determined that we needed at least 20,000 realizations to get a smooth curve fitting with the theory. The shape of the curve for values of SNR between 30 and 40 using BPSK is shown in figure 6.7.

Concerning the throughputs, the curves have similar slopes to the ones presented for a SISO AWGN channel. Nevertheless, the fading the channel

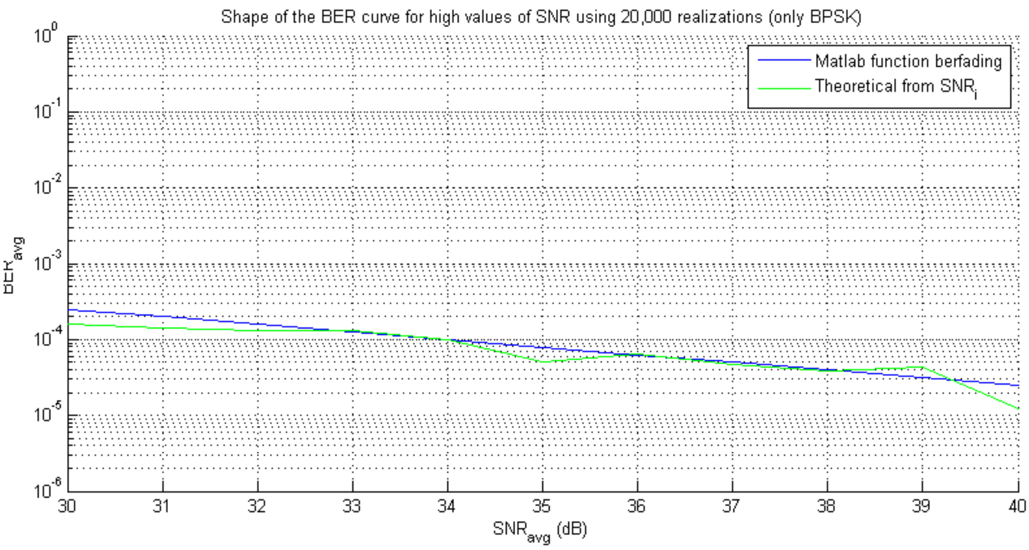

Figure 6.7: Shape of the BER curve at high values of SNR using 20,000 realizations (only BPSK)

is suffering from requires higher values of SNR in order to match the same BER level of an AWGN channel.

6.2 MIMO with perfect CSI

In this section, we will discuss the results obtained with a perfect MIMO communication system (no CSI errors). Some of the code used for the simulations will be presented and commented, including channel modeling, BER calculation and results interpretation. Moreover, some of the pre-processing techniques that have been reviewed earlier in section 4 have been used in our simulations. Concerning MIMO transmissions, we use for all our simulations the Eigenmode transmission scheme as a basis.

Thus, we will begin with a MIMO system using the Eigenmode transmission scheme. Then, we will deal with the case where we use Adaptive Modulation and Coding in addition, and finally, we will study the case where we use both AMC and Water-filling. The results will be presented and interpreted for each case. Then, we will compare them when using different techniques and conclude on the simulations.

6.2.1 Simulations using Eigenmode Transmission scheme

From SISO to MIMO, the program's structure consequently changed. Diagram 6.8 displays the block diagram of the structure of the code used for the following simulations.

Basically, we have a certain number of signals that need to be transmitted over a channel. The channel is composed of several Tx antennas and several Rx antennas. In the simulations, both the size of the system and the number of signals sent can be adjusted. The main difference here lies in the creation of the channel, that here takes the shape of a matrix of dimensions N_{Tx} x N_{Rx}. The creation of the noise also varies with the number of transmitting and receiving antennas. Then, we do the singular value decomposition of the channel and we pre-process the signal. The form of the received signal can be expressed as a combination of equations 4.4 and 3.10 that can be written as:

$$\vec{y} = \mathbb{H}\mathbb{W}\vec{s} + \vec{n} \tag{6.11}$$

The next step is to post-process the signal to recover it rightfully (each parallel stream being independent), as described in Section 4.1 through equations 4.10 to 4.16. From there on, we can determine the BER and the throughputs the same way we did with SISO. Figure 6.9 represents the curve of the BER versus the average SNR for a system with $N_{Tx} = N_{Rx} = 5$ sending five streams (fully-loaded).

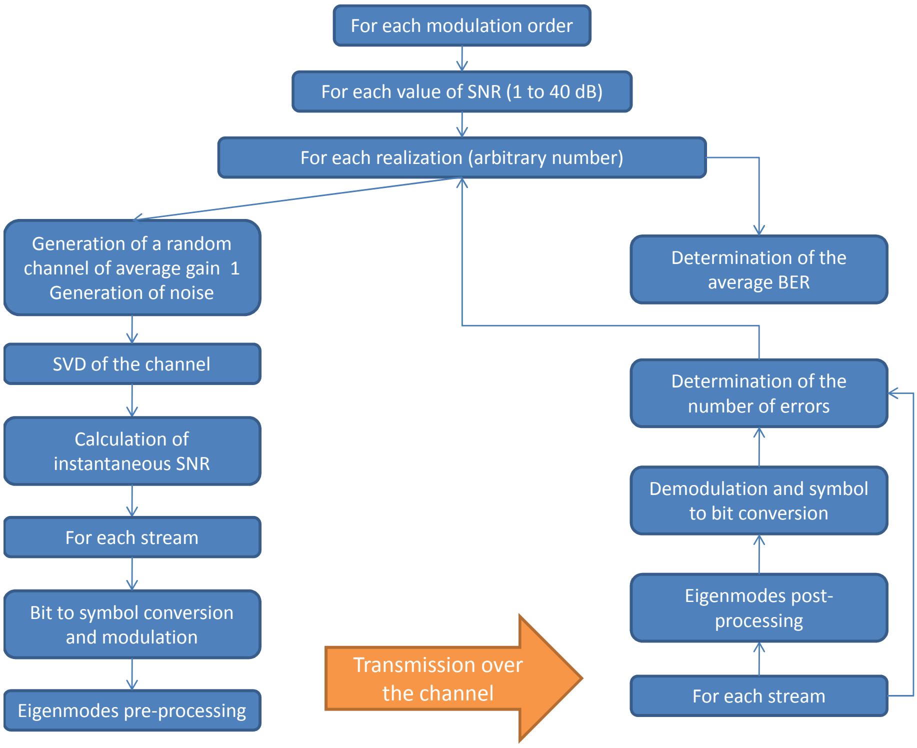

Figure 6.8: Block diagram for a MIMO channel with perfect CSI using Eigenmode transmission scheme

We can see the curves are similar with the ones of a SISO system suffering from Rayleigh fading but there are more errors in the MIMO case. This is due to the total transmit power that is the same for both cases. However, concerning the MIMO, the power is split between the five streams sent over the channel. Each of them has then only one fifth of the power, which results in a higher BER for the whole transmission.

That does not mean a fully-loaded MIMO system is less efficient than a SISO one. Although we noticed it is the case in terms of BER, in terms of throughput, the MIMO system has obviously much higher performances, due to the multiplexing of the streams. We can see this on Figure 6.10.

Influence of the number of streams sent

We are now going to see the influence on the BER of a large system compared to the number of streams to be sent. This situation introduces the same 5-by-5 MIMO system, but this time while sending only one, two and four streams

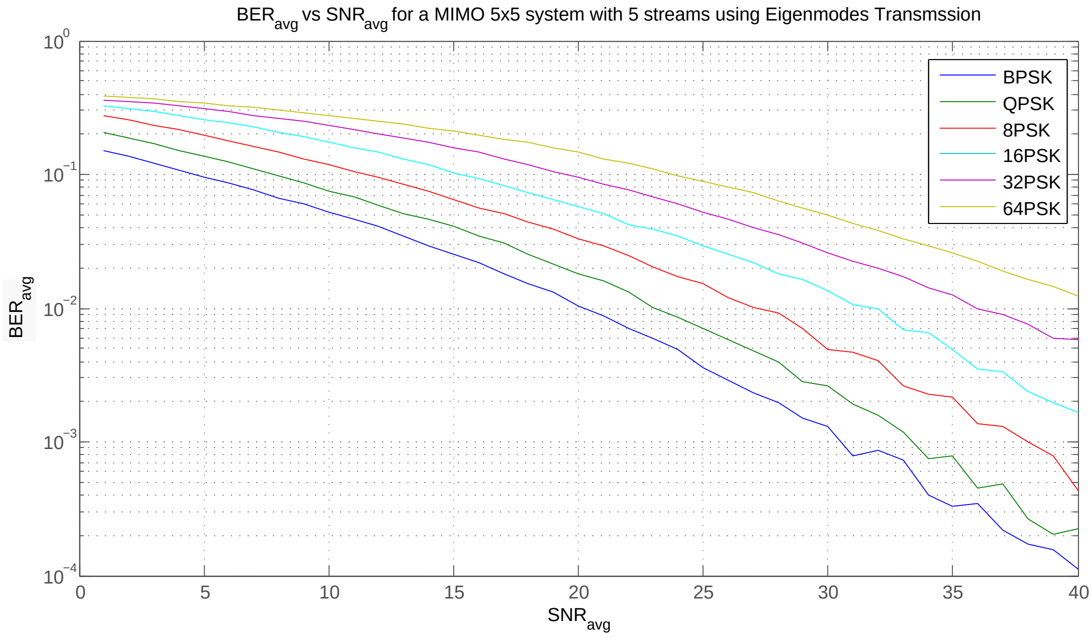

Figure 6.9: Average BER vs. average SNR for a MIMO 5-by-5 system sending 5 streams using Eigenmode transmission

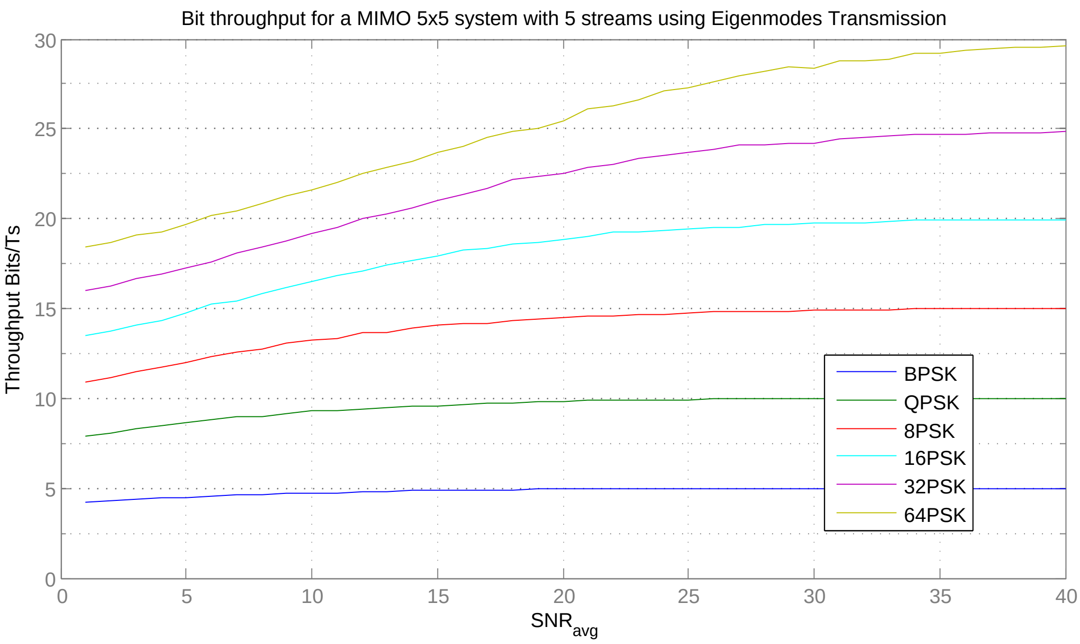

Figure 6.10: Bit throughput for a MIMO 5-by-5 system sending 5 streams

over the channel.

Figure 6.11 displays the average BER with respect to the average SNR for the number of streams mentioned before with different modulations.

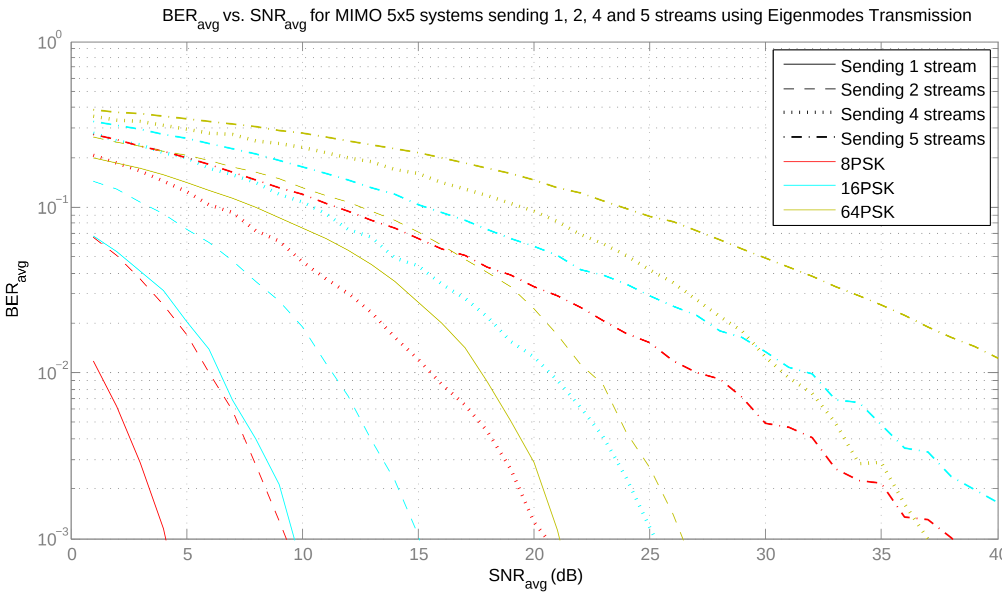

Figure 6.11: Average BER vs. average SNR for a MIMO 5-by-5 system sending 1, 2, 4 and 5 streams using Eigenmode transmission

The red curves represent the BER curves for each case where we send 1, 2, 4 and 5 streams over the channel using 8PSK. The cyan and dark yellow ones are respectively using 16PSK and 64PSK modulations. We easily notice the difference between a fully-loaded system and a 5-by-5 system sending a single stream. We use these higher modulations to do the comparison, since BPSK and QPSK cases are not relevant for the comparison with other system sizes when sending 1 or 2 streams. Indeed, the BER is so low (even at very low SNR) that the curves are barely visible on the scale we are using.

Plain lines are used to display the curves for a single stream sent, dashed lines for 2 streams, dotted lines for 4 streams and finally dash-dotted lines for 5 streams.

We can see that the less streams sent, the better the BER. However, we have already discussed the performance in terms of throughput (available on Figure 6.12) that vary a lot depending on the number of streams sent. Also, in a practical context, the setting up of large systems is costly. Therefore, they should be used in close accordance with the needs.

Let us study the influence of the number of streams on the BER for a fixed modulation. For a 16PSK modulation, when we only send 1 stream, the BER reaches the threshold (10^{-2}) for $SNR_{avg} = 6.45dB$. The threshold is reached for an average SNR of $11.25dB$, $20.65dB$ and $32dB$ when sending 2, 4 and 5 streams respectively. For the first two curves (1 and 2 streams), we notice the slopes are very similar. Nevertheless, the division of the power amongst the transmitting antennas introduces a shift in the BER. Indeed, the antennas all have one fifth of the power at their disposal but from one case to the other, they need to send more or less streams over the channel, but always with the same amount of power. There will obviously be more errors (and the BER values will be shifted) when more streams need to be sent because there is more data to send while the power is not increasing.

Concerning the curves displaying the 4 and 5 streams cases, we can see that they are less steep in addition to the shift mentioned before. The diversity gain (see Section 3.2.2) introduced by the large number of antennas in comparison with the number of streams sent decreases when we start sending a higher number of streams (from 4). Thus, the higher the SNR, the greater the gap between the 1/2 streams and 4/5 streams curves. This is the main point of the next study, the influence of the system size on the BER.

Figure 6.12 represents the throughput curves for the latter systems.

We can see on this figure that, naturally, the more streams sent over the channel, the higher the throughput (especially towards high SNR). Even though the maximum throughput is reached faster (requires lower SNR) for cases where 1 or 2 streams are sent, comparatively, it is less important than for cases where 4 and 5 streams are sent. It is again a matter of how the system should be loaded and what kind of SNR would be available for the transmission. The more streams we send, the higher the throughput, but also the higher the required SNR to reach full capacity (when the throughput equals the maximum throughput for a given modulation order). As illustrated on Figure 6.12, using 8PSK, the maximum throughputs are reached at values of $SNR_{avg} = 3dB$, $9dB$, $21dB$ and $35dB$ when 1, 2, 4 and 5 streams are sent, respectively. The gap between those values remains constant when using higher modulations as we can notice with 64PSK, reaching maximum throughput at $21dB$, $27dB$, $39dB$ and a above $40dB$ for 5 streams sent.

We have seen that the number of streams sent over the channel has a strong influence on the performances both in terms of BER and throughput. Indeed, depending on the system size, a larger number of streams will reduce the BER performance (nearing the SISO Rayleigh channel case) but the throughput ones will be much higher. On the other hand, a smaller number

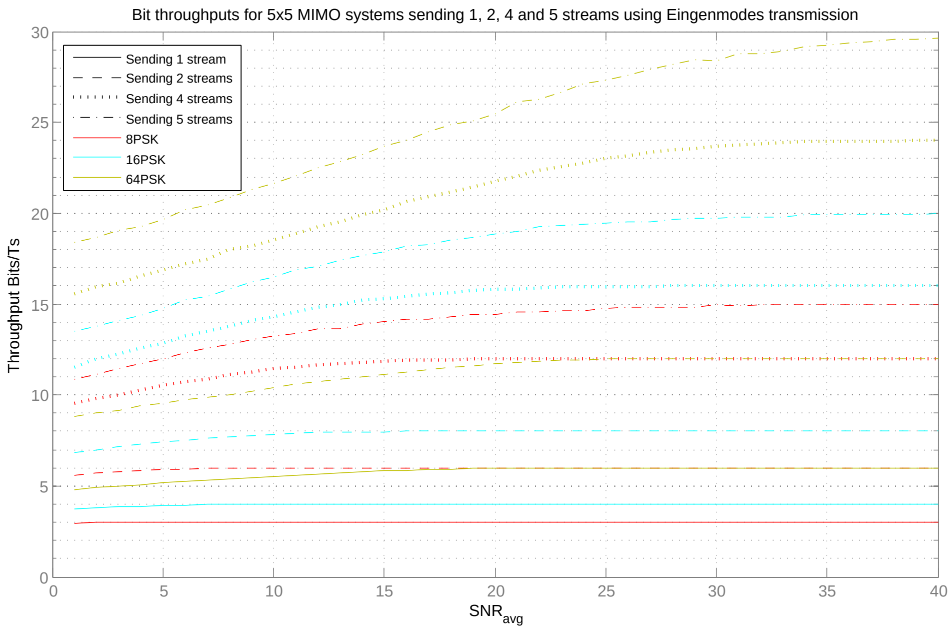

Figure 6.12: Bit throughput for 5-by-5 MIMO systems sending 1, 2, 4 and 5 streams using Eigenmode Transmission

of streams will drastically increase the BER performances, but to the expense of the throughput, along with the amount of data sent.

Influence of the system size

We are now going to study the influence of the system size on overall performances. The comparison will be led between SISO, MIMO 5-by-5 and MIMO 8-by-8 fully-loaded systems.

Figure 6.13 displays the BER curves for those systems using BPSK, 16PSK and 64PSK.

The SISO case remains the best in terms of BER performance. Also, this difference in BER barely varies with different modulations. Indeed, at $SNR_{avg} = 20dB$, for a BPSK modulation in SISO, $BER_{avg} = 2.3.10^{-3}$ whereas in MIMO 8x8, $BER_{avg} = 1.4.10^{-2}$, so to say a difference of $1.17.10^{-2}$. For 16PSK modulation at the same value of SNR, $BER_{avg} = 3.2.10^{-2}$ in SISO and $BER_{avg} = 5.6.10^{-2}$ in MIMO 8x8, a difference of $2.4.10^{-2}$. And finally, concerning 64PSK, $BER_{avg} = 1.3.10^{-1}$ for SISO and $BER_{avg} = 1.5.10^{-1}$ for MIMO, a difference of 2.10^{-2}. The curves are also rather parallel from one system to the other, it means these fully-loaded systems have the same diversity order with respect to number of streams sent.

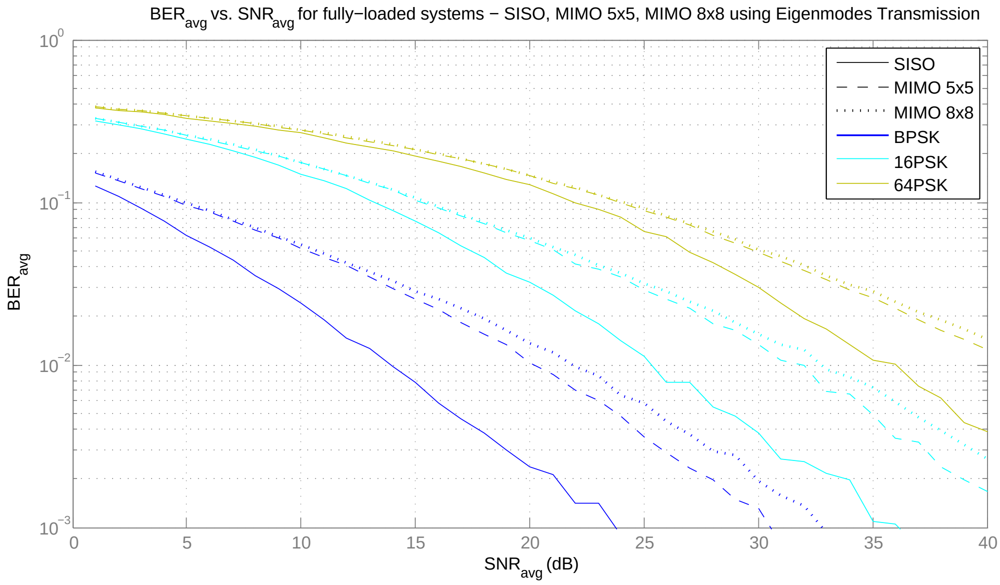

Figure 6.13: Average BER vs. average SNR for SISO, MIMO 5x5 and MIMO 8x8 fully-loaded systems using Eigenmode Transmission

We can deduce that the system size has actually the same impact on the different modulations at a fixed SNR. However, the BER is generally lower for a small system than for a large one, because of what we mentioned earlier with the transmit power being divided among the antennas.

We will now discuss the influence of the system size on the throughput curves, available on Figure 6.14.

As we have seen throughout this section, the throughput increases along with the number of streams sent and the modulation order. The BER performances being better for smaller systems, the maximum throughput for each modulation is reached earlier than for larger systems.

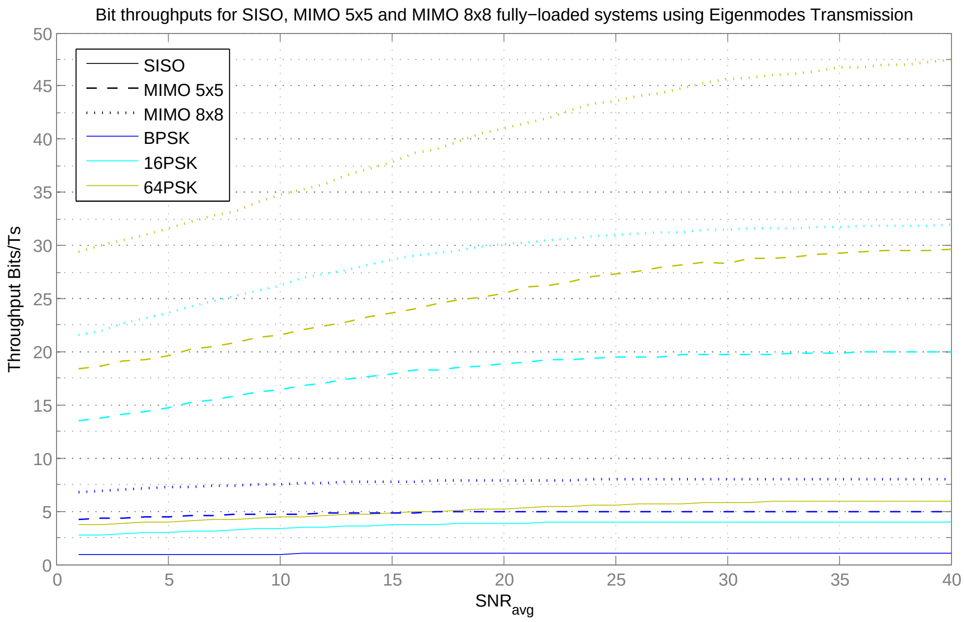

Figure 6.14: Bit throughputs for SISO, MIMO 5x5 and MIMO 8x8 fully-loaded systems using Eigenmode Transmission

6.2.2 Simulations using AMC pre-processing

As we discussed in the theoretical section 4.2, the AMC requires the setting of a range of modulation levels to respect a fixed threshold. The range values are obtained from the BER curves of a SISO AWGN channel with perfect CSI. The goal of AMC pre-processing is to maximize the throughput while obeying the BER constraint. The block diagram of our code for a MIMO channel using AMC pre-processing can be seen on Diagram 6.15.

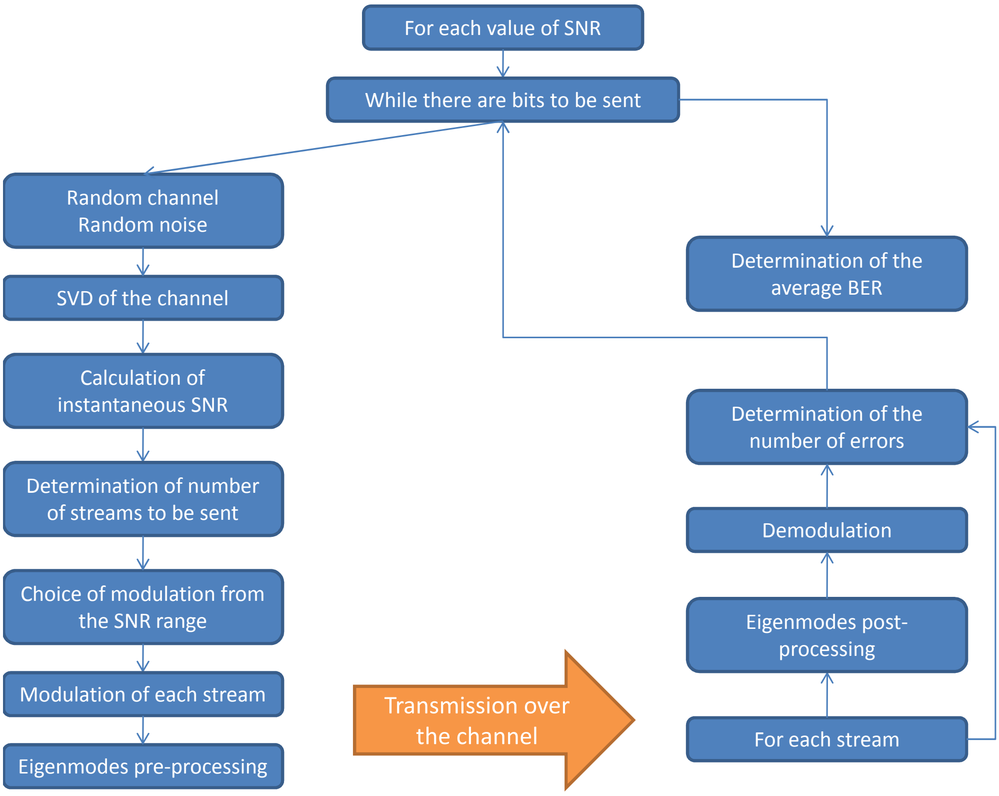

Figure 6.15: Block diagram for a MIMO channel with perfect CSI using AMC

We have studied this pre-processing method for two different BER thresholds, 10^{-2} and 10^{-3}. Figure 6.16 displays the average BER versus average SNR curve for a fully-loaded 5-by-5 MIMO system using AMC (with both thresholds) in addition to the Eigenmode transmission scheme.

We can see that the values of BER respect the thresholds that have been set in both cases. The throughput curves (seen on Figure 6.17) allow us to see that throughout the simulation, the number of bits sent increases while the BER remains under the threshold. It emphasizes the choice of modulation

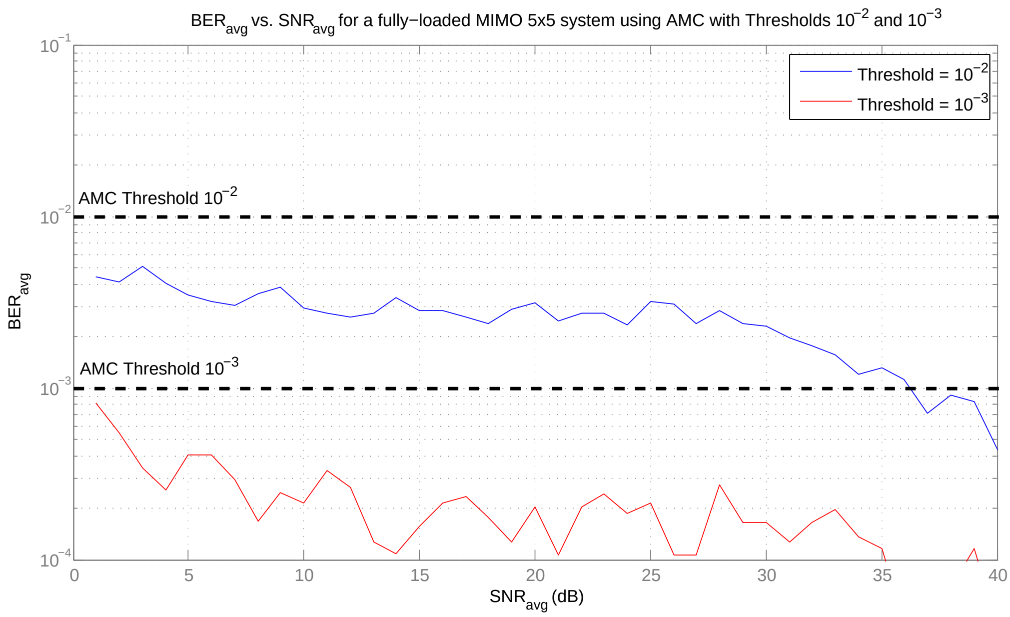

Figure 6.16: Average BER vs. average SNR for a fully-loaded 5-by-5 MIMO system using AMC

that occurs depending on the instantaneous SNR. Using higher modulations, we send more bits during the same period of time.

We can notice that the throughput is higher for a BER target of 10^{-2}. This is due to the modulation ranges varying according to the threshold set. Indeed, Table 4.1 from Section 4.2 displays those ranges for a BER threshold of 10^{-2}. Let us compare them with the ones for a threshold of 10^{-3}, available on Table 6.1.

SNR range(dB)	Under 6.8	6.8 to 9.7	9.7 to 14.7	14.7 to 20.3
Modulation	No signal	BPSK	QPSK	8PSK

SNR range(dB)	20.3 to 26.1	26.1 to 31.9	31.9 and above
Modulation	16PSK	32PSK	64PSK

Table 6.1: Modulation used for AMC with respect to the SNR range for a BER threshold of 10^{-3}

As we could expect, the minimum value of SNR required to obey the BER threshold is higher for a threshold of 10^{-3} than 10^{-2}.

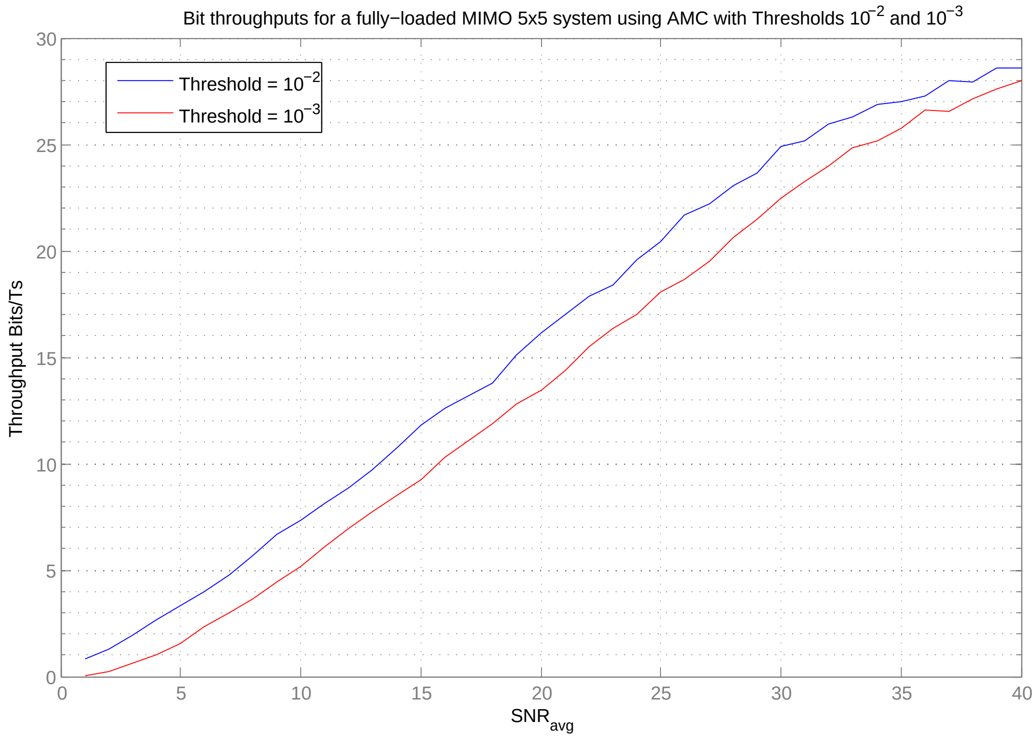

Figure 6.17: Bit throughputs for a fully-loaded 5-by-5 MIMO system using AMC

On Figure 6.17 appear what we could call bumps at certain values of SNR. Indeed, each time the SNR reaches a value used to set the levels of modulation, there is a noticeable increase in the throughput. Also, those bumps do not take place at the same values of SNR for the two thresholds set, since the ranges used vary with respect to the threshold. This again comes down to the influence of the threshold on the modulation ranges, shifting the values from which we can increase the modulation orders. Next section 6.2.3 discusses the use of AMC along with Water-filling, in which we study the influence of AMC with and without Water-filling on different parameters such as modulation used, throughput and BER.

6.2.3 Simulations using AMC and Water-filling pre-processing

The Water-filling processing is known to be really efficient only when AMC is also used. This is the reason why we are only focusing our results presentation on Water-filling coupled with AMC.

Effect of the Water-filling on a given modulation order

We have seen in Section 4.2 that AMC chooses the best modulation depending on the instantaneous SNR. Combined with Water-filling, AMC leads to an even greater increase of the system throughput. Indeed, the power is allocated to the channels in a descending order of quality, which allows the AMC to use higher orders of modulation. This mechanism can be perfectly seen on Graph 6.18 representing the probability of using a given modulation at a given average SNR.

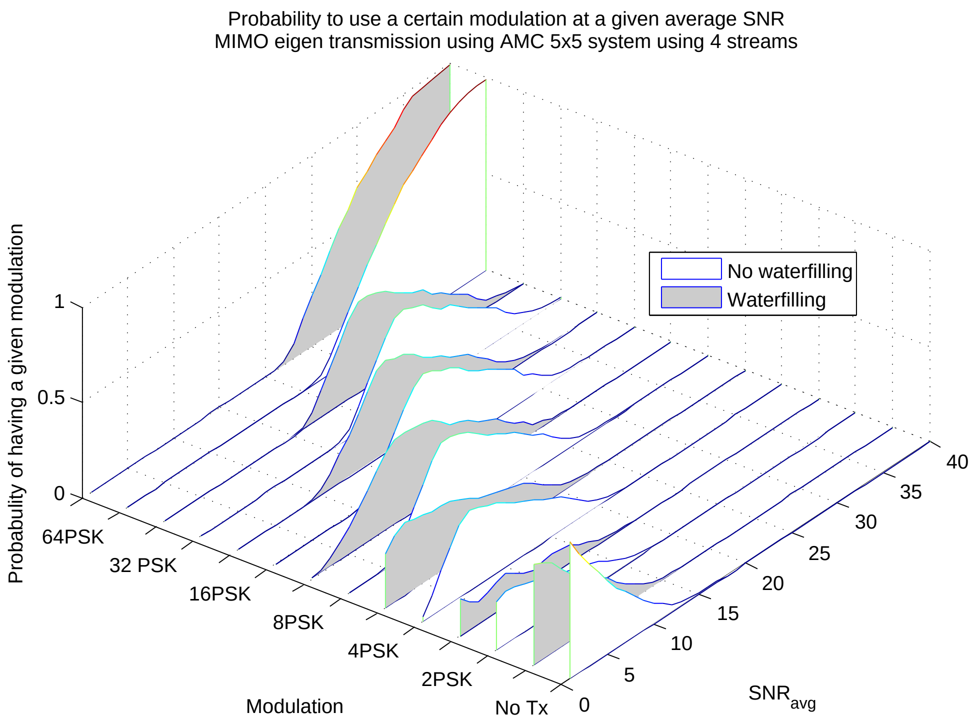

Figure 6.18: Probability of using a given modulation in AMC MIMO context

We can notice that Water-filling decreases the probability of non-transmitting streams for low average SNR (under 4.3dB) and increases the probability of transmitting with higher modulation for a given average SNR. The 2PSK modulation is less used at the expense of a higher modulation such as 4PSK.

Nevertheless, this effect is not present above 32PSK, where the probability of choosing a certain modulation is the same without Water-filling.

Effect of Water-filling on throughput

The effect on the throughput is straightforward. We have seen on Figure 6.18 that the modulation is statistically increased for a given SNR and as the AMC BER threshold is respected (here 10^{-2}), the throughput is higher with water-filling for low SNR. These effects can be seen on Graph 6.19, where each is represented.

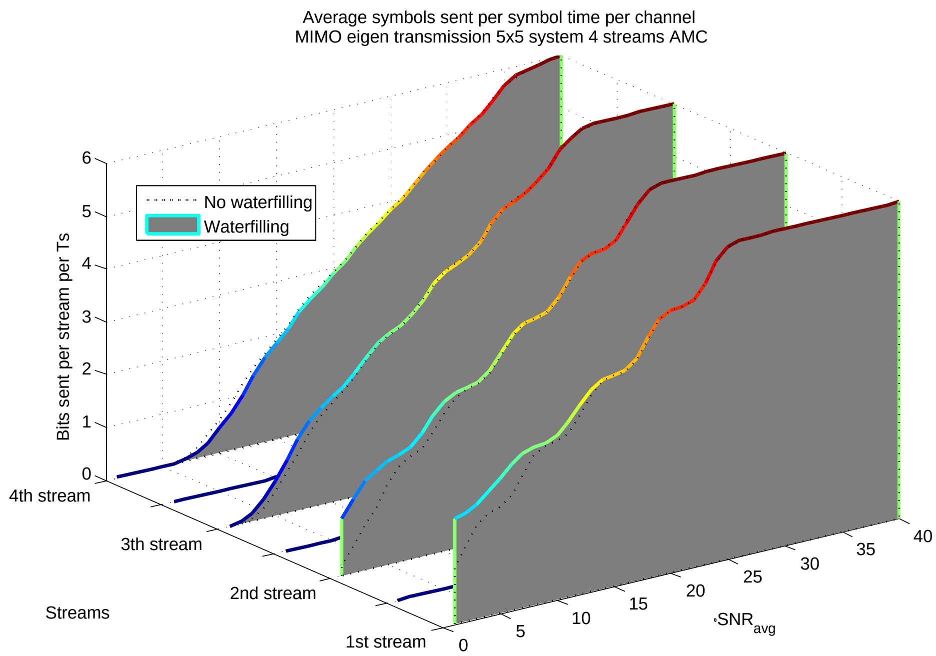

Figure 6.19: Average bits sent per symbol time per channel with MIMO transmission using Water-filling

As we have seen before, the SVD decomposition is sorting the Eigenvalues in descending order, which means the first streams are much stronger. We can see the effect of water-filling on the 3 first streams for low average SNR : the number of bits sent per symbol time per stream is higher, on the contrary, the 4th one is using lower modulation due to the poor quality of the link.

The total throughput is displayed on graph 6.20. The effect of Water-filling is visible at low SNRs. We can deduce that it is interesting only for low average SNR.

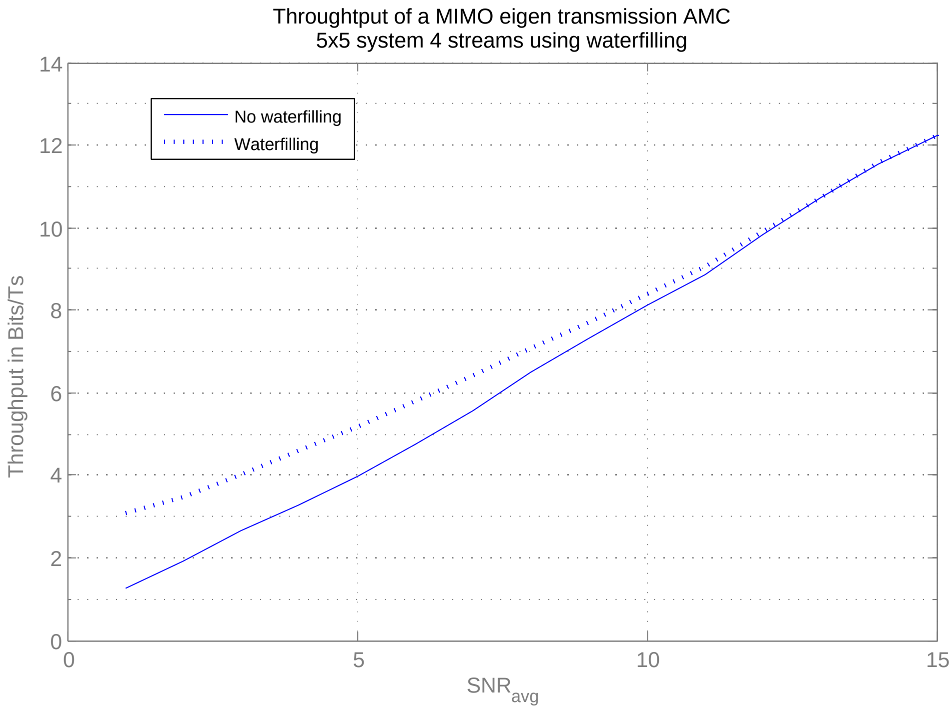

Figure 6.20: Throughput of a MIMO 5x5 system sending 4 streams using Eigenmode transmission with AMC and Water-filling

Effect of Water-filling on BER

On Figure 6.22, with water-filling, we still observe the waves due to the modulation changes. SISO AWGN curves have been plotted to underline the AMC effect. These are the curves that have been used to set the AMC threshold. It can be noticed that the Water-filling curve and normal curve are woven. The nodes are the AMC BER thresholds.

Two theories can be drawn up to explain this woven phenomenon:
The graph 6.22 displays two possible situations in Water-filling/AMC processing. With Water-filling, we increase the power on certain streams, we increase the instantaneous SNR, AMC decision use higher modulation leading to a change of BER.

- 1^{st} situation: The jump noticed in Water-filling/AMC processing leads to a transmission with a higher BER for a given SNR than without Water-filling.
- 2^{nd} situation: The jump noticed in Water-filling/AMC processing leads to a transmission with a lower BER for a given SNR than without

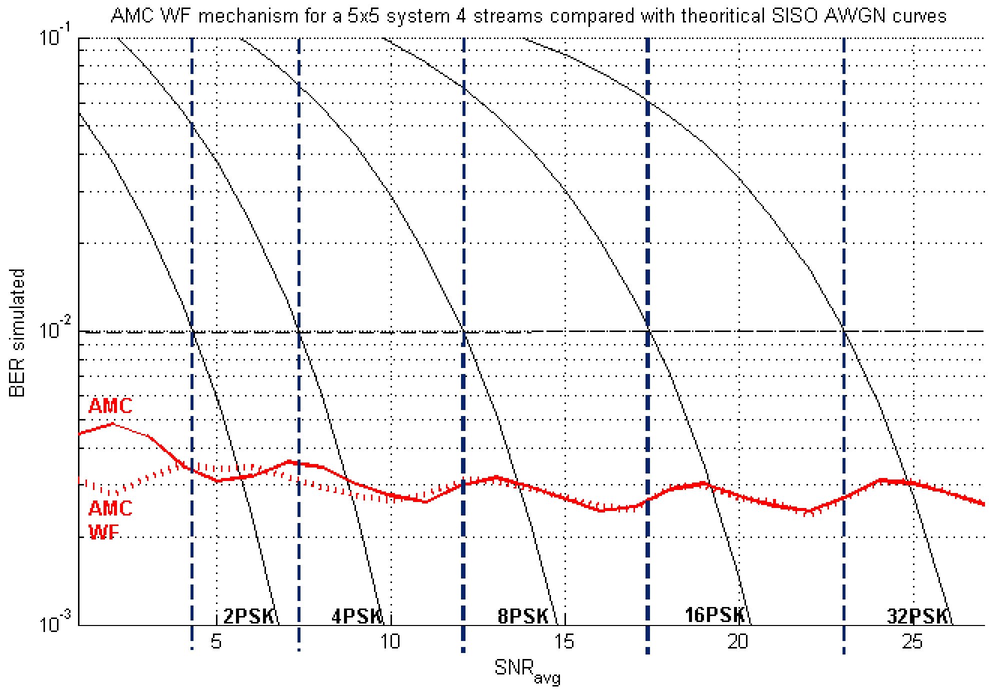

Figure 6.21: AMC results illustrated with SISO theoretical curves

Water-filling.

Regarding the throughput (Figure 6.20), the performance is clearly related to the BER as we are not using the packet transmission mechanism. The effect of the Water-filling is not obvious, however, it is more efficient for low values of SNR.

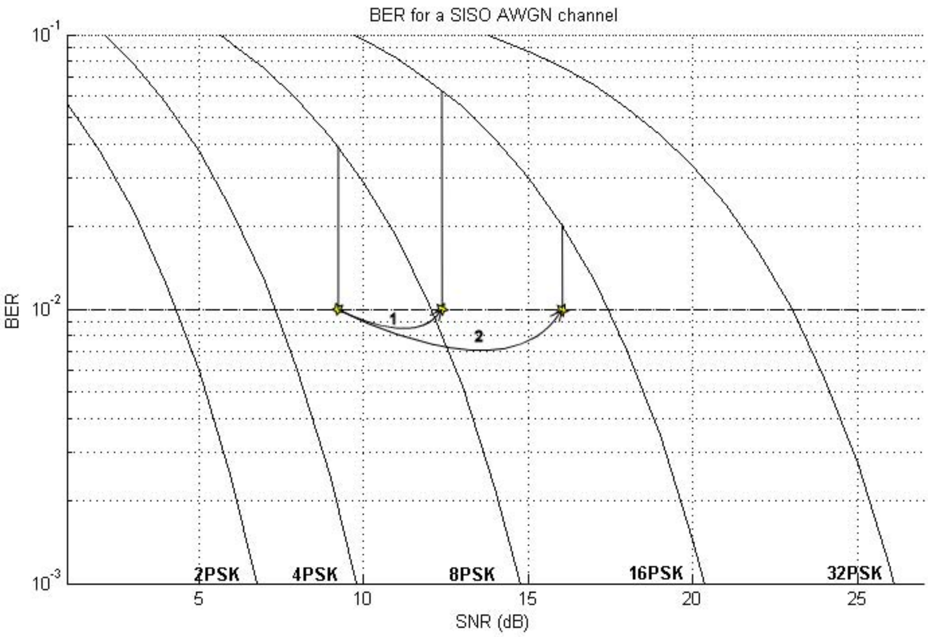

Figure 6.22: BER for AWGN fading : explanation of woven curves when using AMC

6.3 MIMO with imperfect CSI

The aim of the previous simulations was to establish a model of communication system. Using this basis, the notion of channel error can be implemented. As discussed before, the simulation analysis is focused on noise and Doppler estimation errors.

The most complex communication model simulated in the project is the MIMO Eigenmode-transmission using AMC and Water-filling. It is not straightforward to study the impact of a misestimated channel. Some intermediate steps are necessary to reach a good analysis and interpretation of the effects. Each type of error is simulated independently, looking at the impact on a simple MIMO transmission with a different fixed modulation, without Water-filling. Then AMC is introduced with and without Water-filling.

The simulation have been made with a MIMO 5x5 system sending 4 streams with CSI errors at both sides (Tx and Rx). The influence of CSI errors at only one side is studied in the following sections. The estimation model chosen is the training sequence approach (see section CSI 3.3).

The block diagram 6.23 explains the simulation process used to simulate CSI errors in general (this is an example of CSI at both side, Tx and Rx).

6.3.1 Channel Noise Error

As seen in the theoretical section, the noise could be simulated using two methods. The simple one describes the quality of the estimation as constant even if we increase the quality of the transmission. On the contrary, the advanced method is taking into account the SNR of the transmission.

Simple channel estimation undergoing noise

As seen in section 3.3,the misestimated channel $\hat{\mathbb{H}}$, taking into account only noise error, can be described as :

$$\hat{\mathbb{H}}_{no} = \mathbb{H} + \sigma_{\mathbb{H}_{error}} \mathbb{W} \tag{6.12}$$

$\mathbb{W}$ is a matrix of dimensions N_{Tx} x N_{Rx} with zero-mean circularly symmetric complex Gaussian (ZMCSCG) entries and variance 1.
$\sigma_{\mathbb{H}_{error}}$ is the standard deviation of the CSI error.
We assume the reciprocity of the channel, which means it assumes the channel

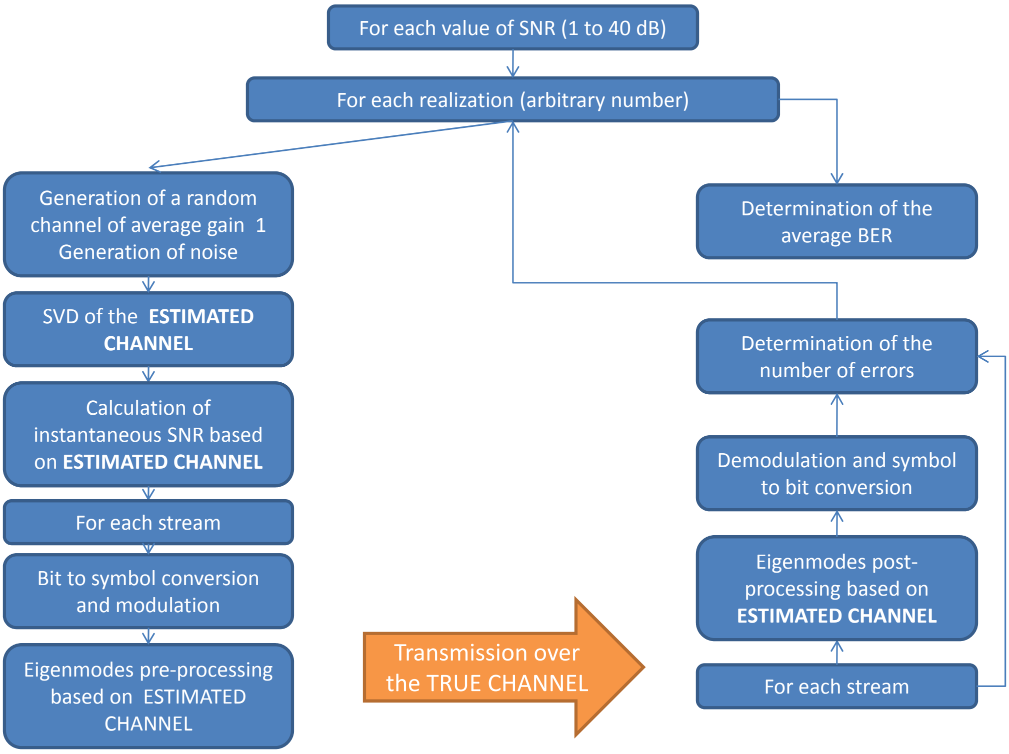

Figure 6.23: General block diagram of the transmission with imperfect CSI

from the transmitter to the receiver is approximately the same as the channel from the receiver to the transmitter.

Effect on modulation of channel estimation undergoing noise

A misestimated channel due to noise has a stronger effect on higher modulations. It can be explained by the intrinsic nature of modulation mechanisms. Indeed, since the symbols in the constellation size are closer, a misestimation of the channel easily leads to a wrong interpretation of the symbols.

On the graph 6.24, an irreducible BER can be observed. An irreducible BER represents the lowest level of BER that can be reached. For example, using 64PSK, the irreducible BER is 0.2 for a $SNR_{Herr} = 15dB$.

It can be explained mathematically with a SISO simplification. Indeed, we can consider in our case that each stream is an independent SISO stream

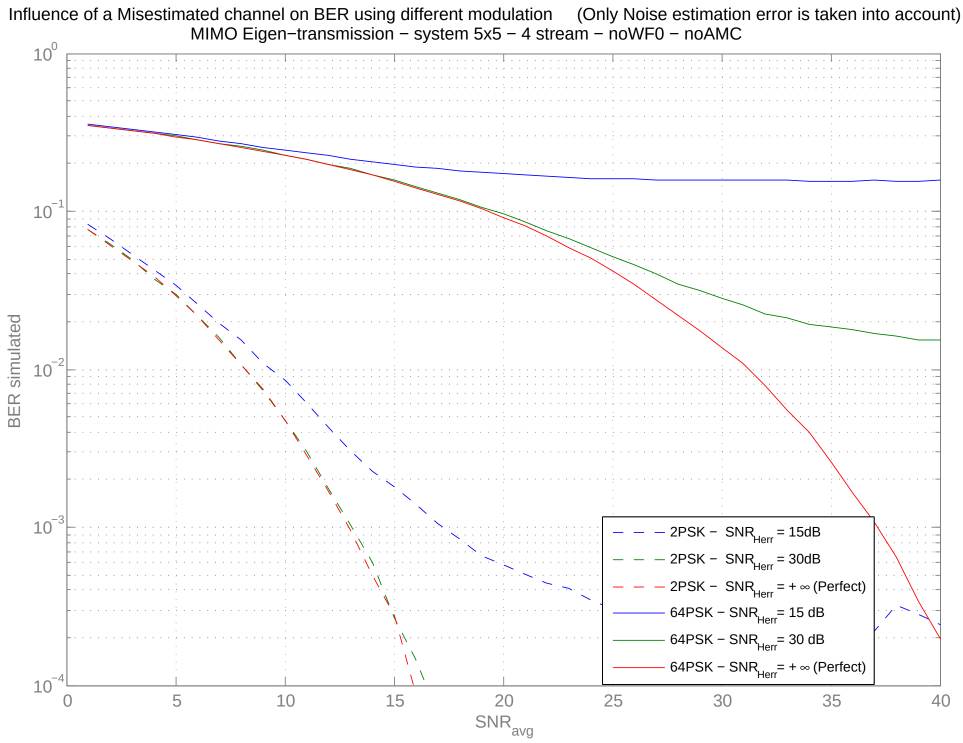

Figure 6.24: Influence of a misestimated channel (noise only) on different modulations with CSI errors at Tx and Rx

because we are not taking into account ISI and each noise is independent. Let us take the basic formula of transmission including misestimation of the channel $\delta h_i.\vec{x}$ for one stream:

$$\vec{y_i} = h_i.\vec{x} + \delta h_i.\vec{x} + \vec{n_i} \tag{6.13}$$

The SNR is defined as :

$$\begin{aligned} if \quad \delta h_i = 0 \quad SNR = \frac{\|h_i\|^2.E(|x|^2)}{\sigma_{n_i}^2} \\ if \quad \delta h_i \neq 0 \quad SNR = \frac{\|h_i\|^2.E(|x|^2)}{\sigma_{n_i}^2 + \|\delta h_i\|^2} \end{aligned} \tag{6.14}$$

If the number of realizations tends towards infinity, $\|h_i\|^2 \to 1$ and $E(|x|^2) \to 1$ due to their Gaussian properties. So the SNR becomes :

$$\begin{aligned} if \quad \delta h_i = 0 \qquad SNR = \frac{1}{\sigma_n^2} \\ if \quad \delta h_i \neq 0 \quad SNR = \frac{1}{\sigma_n^2 + \|\delta h_i\|^2} \end{aligned} \tag{6.15}$$

On this graph, the SNR is increasing with a constant power which means $\sigma^2_{n_i}$ tends towards 0. The irreducible SNR for $\delta h_i \neq 0$ is :

$$SNR_{irred} = \frac{1}{\|\delta h_i\|^2} \tag{6.16}$$

The irreducible SNR is linked to the degree of error made.

Effect on AMC of channel estimation undergoing noise

The AMC is as expected impacted for high SNR as we are using high modulations (Graph 6.25).

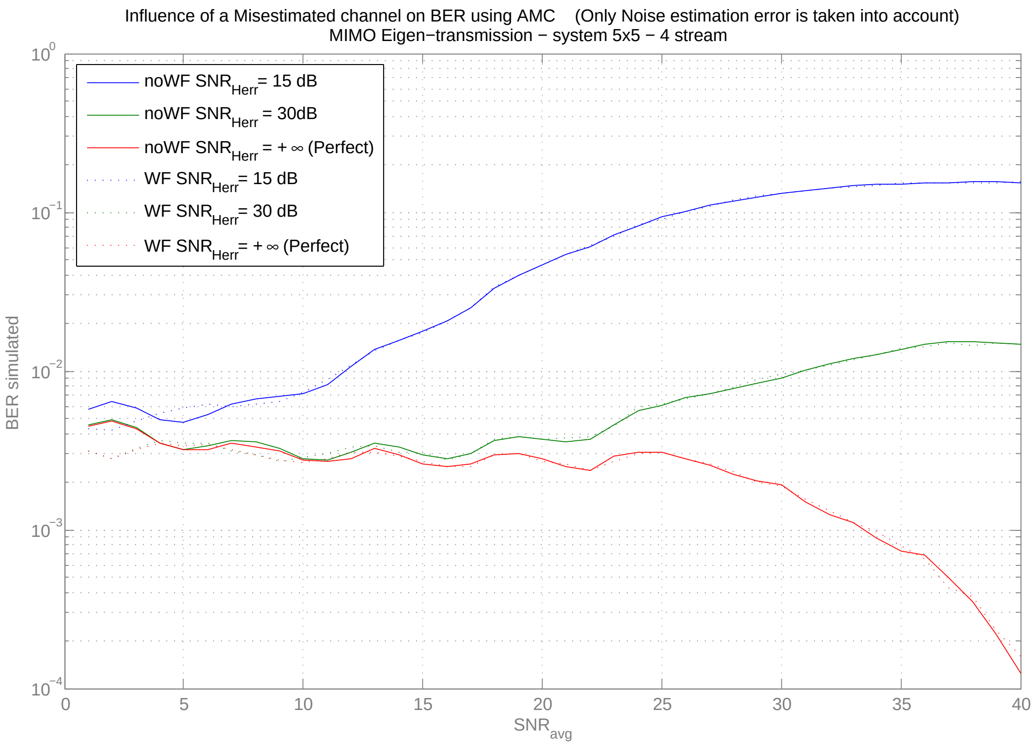

Figure 6.25: Influence on BER of a misestimated channel (simple noise only) on AMC

A channel SNR above 30dB is necessary to maintain the BER below the AMC threshold.

Relative Noise Estimation

The relative noise estimation is a more advanced representation using the training based approach. The error is related to the quality of the estimation directly influenced by the length of the training sequence as expressed on equation 6.17:

$$SNR_{\mathbb{H}_{est}} = SNR_i + T = \frac{1}{\sigma^2_{\mathbb{H}_{error}}} \tag{6.17}$$

where $SNR_i(dB)$ is the average channel SNR,
$T(dB)$ is the quality of the estimation related to the length of the training sequence ($T = \infty$ means perfect estimation).

Effect on modulation of channel estimation undergoing relative noise

The throughputs of fixed modulations are impacted at low SNR (graph 6.26) by relative noise errors but when the average SNR of the transmission increases, the value in dB of the estimated channel T (see equation 6.17) becomes high enough to cancel the effect of the noise error estimation. Also we noticed that high modulations order are more impacted.

Effect on AMC of channel estimation undergoing relative noise

We can see on graph 6.27, a MIMO system with CSI errors at Tx and Rx that the effect of the relative noise above 10 dB is similar to the one with simple noise. The effect of the relative noise on AMC is interesting. Indeed, at low SNRs, throughputs of the transmission suffering from Tx and Rx estimation errors are higher than the perfect channel. However, above 10dB, the effect is similar to the simple noise error. Then, due to the relative noise, the effect vanishes above 40dB (curves converge).

The effect below 10dB can be explained by the nature of the relative noise. The value of $\sigma_{\mathbb{H}_{error}}$ is close to 1 at low SNRs, so the mean square value of $\mathbb{N}\sigma_{\mathbb{H}_{error}}$ is close to 1. As we have seen, the relative noise is expressed as :

$$SNR_{\mathbb{H}_{est}} = SNR_i + T = \frac{1}{\sigma^2_{\mathbb{H}_{error}}} \tag{6.18}$$

We know that the mean square value of a rayleigh channel is 1.

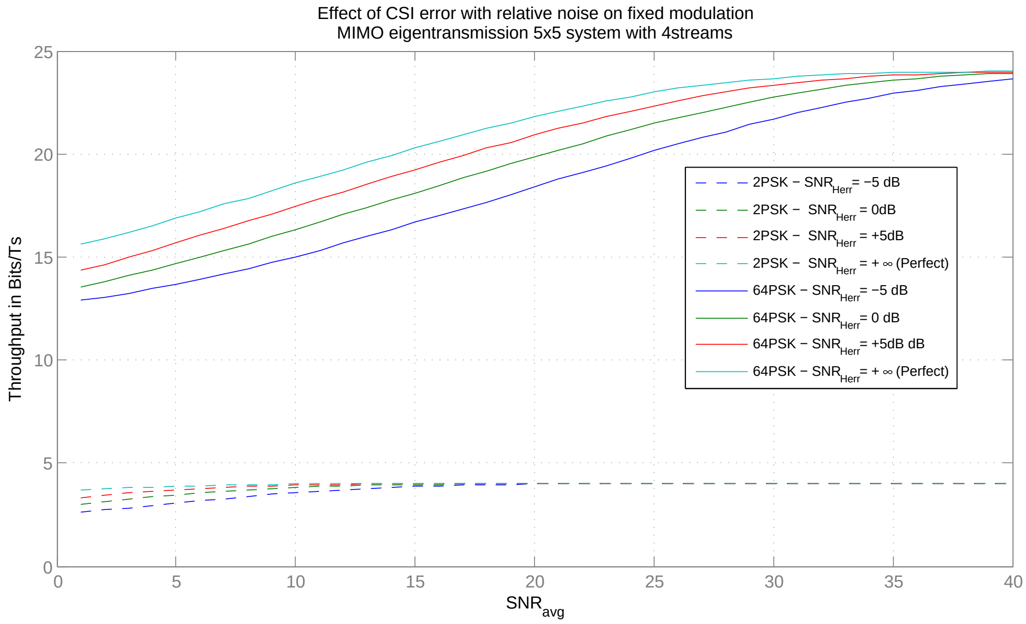

Figure 6.26: Influence on throughput of a misestimated channel (relative noise only) on different modulations

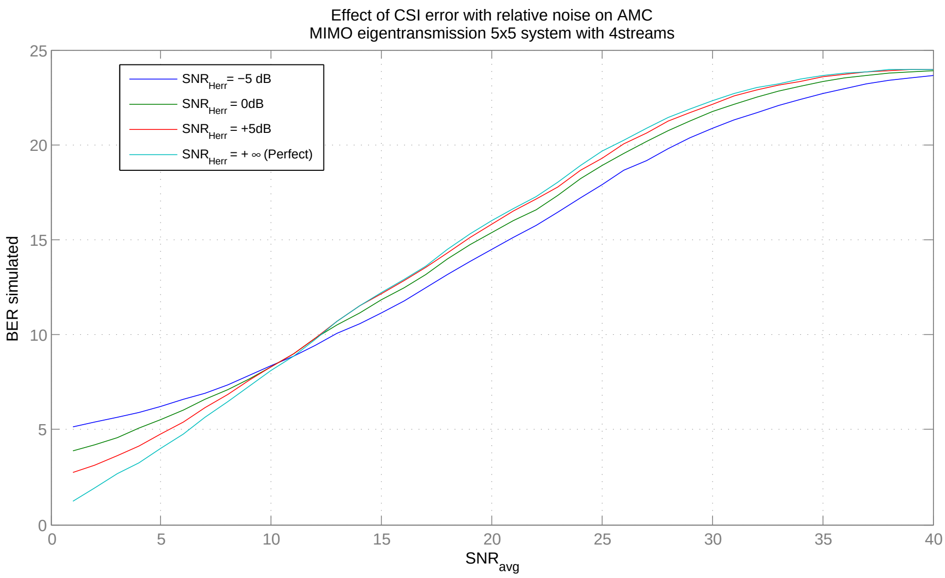

Figure 6.27: Influence of a misestimated channel (relative noise only) on AMC

So the mean square value of the misestimated channel with relative noise will be close to 2 at low SNR :

$$E[\mathbb{H}_{error}{}^2] = E[\mathbb{H}_{error}{}^2] + E[\mathbb{W}\sigma_r{}^2] = 1 + 1 = 2 \tag{6.19}$$

As explained previously, the AMC is based on the instantaneous SNR, which is based on the eigenvalues extracted from the channel estimated. As the channel has a higher mean square value, the eigenvalues are greater and the instantaneous SNR is overvalued. The AMC is based on SNR ranges to determine the modulation. Due to the overvalued SNR, the algorithm is choosing higher modulation orders than the ones it should usually choose. So we can see on BER curves of SISO channel with imperfect CSI (graph 6.28) that the errors are greater, but the throughput (graph 6.29) is higher due to the increase of the data rate.

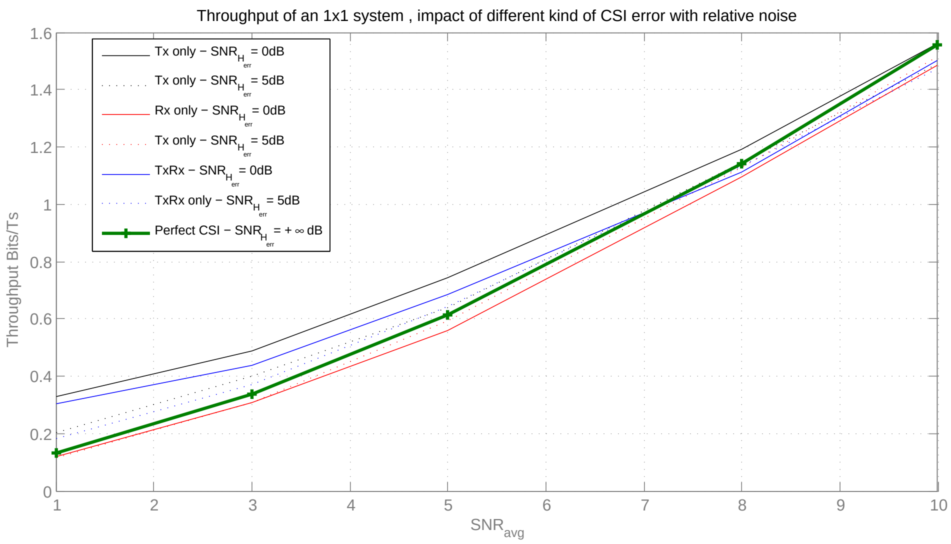

Figure 6.28: Influence on throughput of a misestimated channel (relative noise only) on SISO

This phenomenon can be explained in details, for example, for a SNR around 7.3dB (value from which AMC switches to QPSK):

- For a high number of channel errors realization, the (post-processing) SNR will be overestimated, so to say SNR (with CSI relative noise error) $>$ 7.3dB while the actual is less than 7.3 dB.
- When the SNR is underestimated and below 4.3dB, the throughput for impefect CSI $<$ throughput with perfect CSI. However the number of

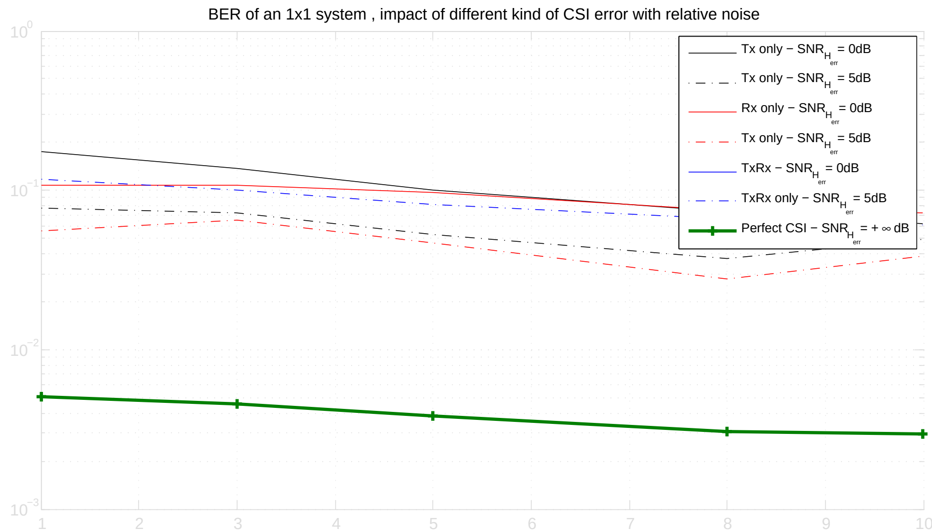

Figure 6.29: Influence on BER of a misestimated channel (relative noise only) on SISO

occurence of this case is lower than overestimation case when SNR_{avg} is 7.3dB. Only transmissions with CSI imperfection at Tx or at Tx and Rx are impacted. The Rx only errors are not impacted, as the estimation of the channel at the transmission is correct.

The overvalued instantaneous SNR theory is confirmed by the graph 6.30

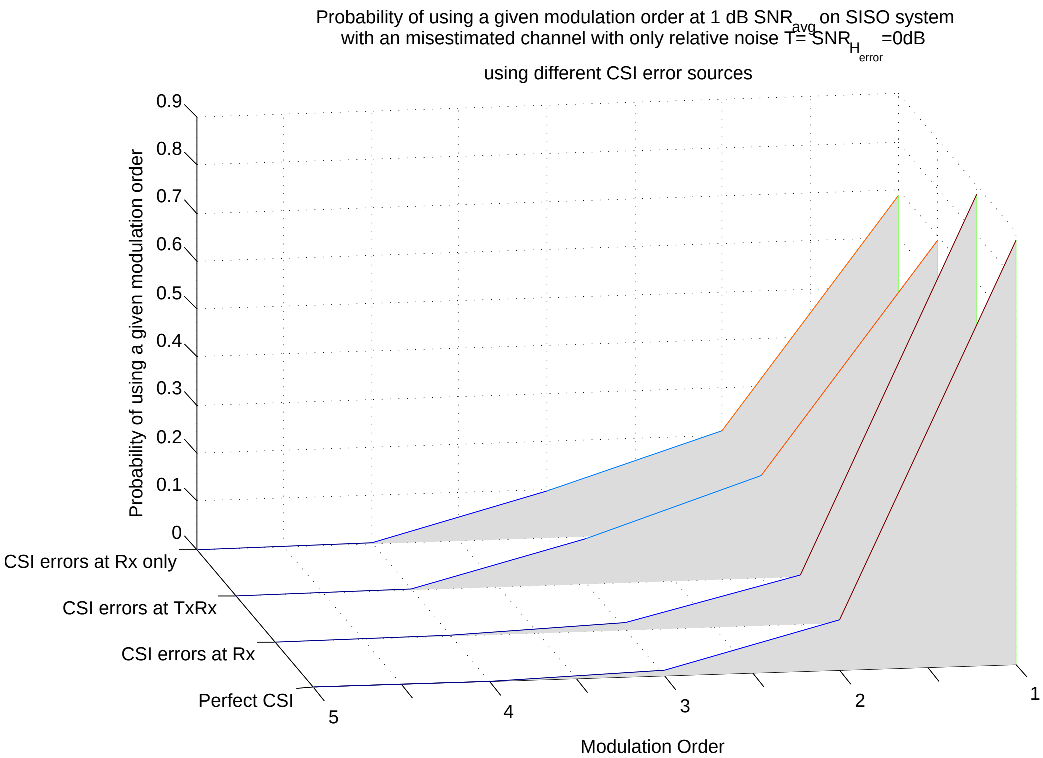

Figure 6.30: Probability of using a given modulation order at 1 dB SNR_{avg} on SISO system with an misestimated channel with only relative noise $T = SNR_{H_{error}} = 0dB$ using different CSI error sources

6.3.2 Channel Doppler Error

As seen in the theoretical section, the simplified representation of the error induced by the Doppler effect can be done using the parameter ρ, the coefficient of correlation between $\hat{\mathbb{H}}$ and $\mathbb{H}$. This representation supposes we are using the training sequence approach. The mathematical representation can be noted as :

$$\hat{\mathbb{H}}_{do} = \rho\mathbb{H} + \sqrt{1-\rho^2}\mathbb{W} \tag{6.20}$$

$\mathbb{W}$ is a matrix of dimensions N_{Tx} x N_{Rx} with zero-mean circularly symmetric complex Gaussian (ZMCSCG) entries with variance 1.

As expressed previously, the correlation ρ can be expressed in function of the distance traveled δ_l between two measures:

$$\rho(\delta_l) = J_o\left(2\pi\frac{\delta_l}{\lambda}\right) \tag{6.21}$$

For example at 3Ghz and at 5Ghz, for a correlation of 0.9 according to the curves 5.2 and to the formula 5.9, the distance traveled by the receiver in movement is respectively 1.76 cm and 1.05 cm.

Effect on modulation of Doppler error estimation

The misestimated channel due to Doppler errors has a similar effect on BER performance as noise errors (see graph 6.31). We also notice the irreducible BER with a certain floor. Notwithstanding, the effect seems to impact more the estimation for low SNR.

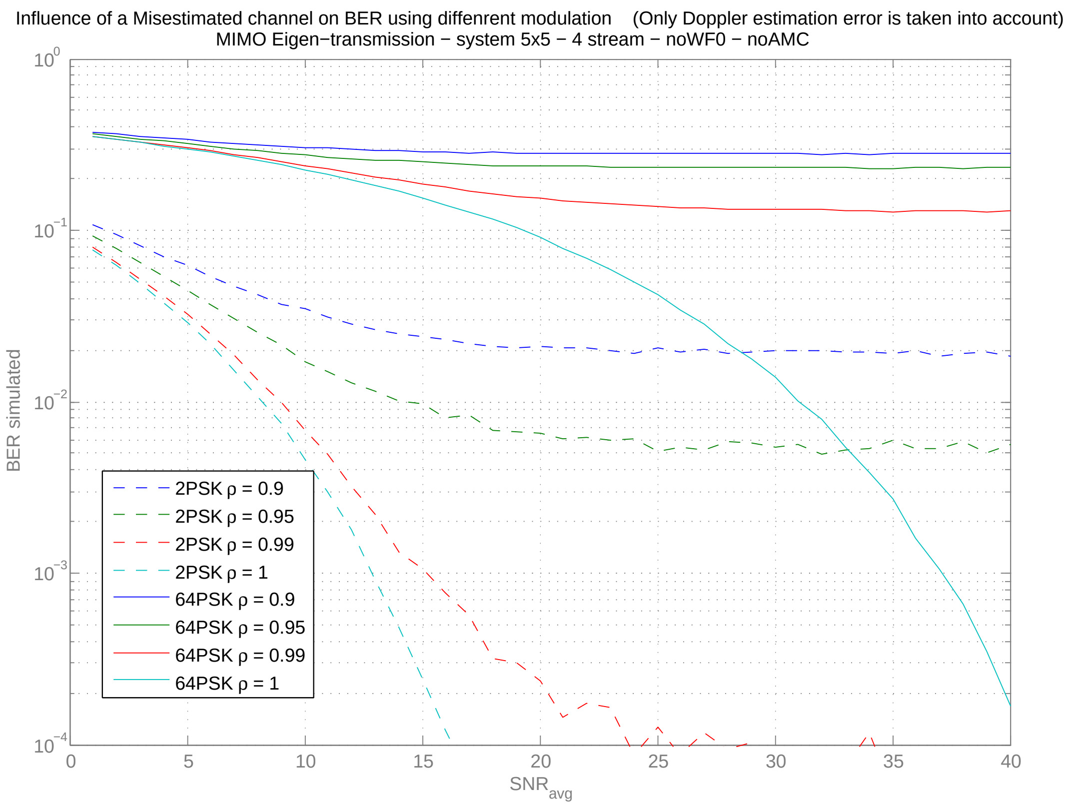

Figure 6.31: Influence of misestimated channel (relative noise only) on AMC

Regarding the throughputs, we can notice that at fixed modulation, even at high SNR, the effect of the misestimation is visible. Moreover, high modulations are more impacted by the correlation: for example a correlation of 0.99 has a negligible effect for SNR higher than 20dB using 2PSK while the effect cannot be neglected using 64PSK.

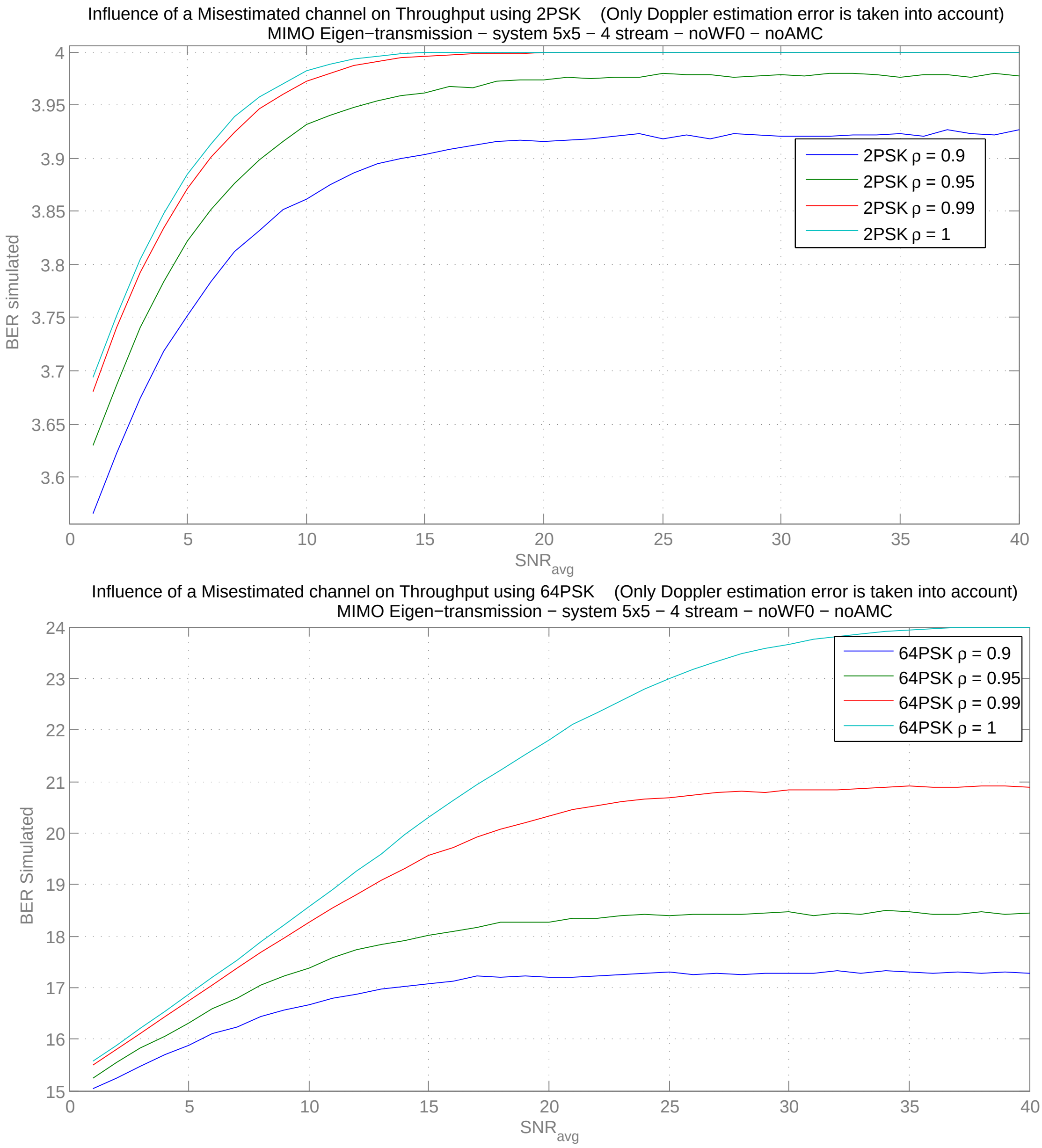

Figure 6.32: Influence of a misestimated channel (Doppler only) on fixed modulations. On top, BPSK and on the bottom, 64PSK

Effect on modulation of Doppler error estimation

As seen previously, the effect on AMC (graph 6.33) is really similar as simple noise effect. The correlation has a strong effect on high modulations. The coefficient has to be really close to 1 to achieve a correct AMC transmission and reasonable throughput.

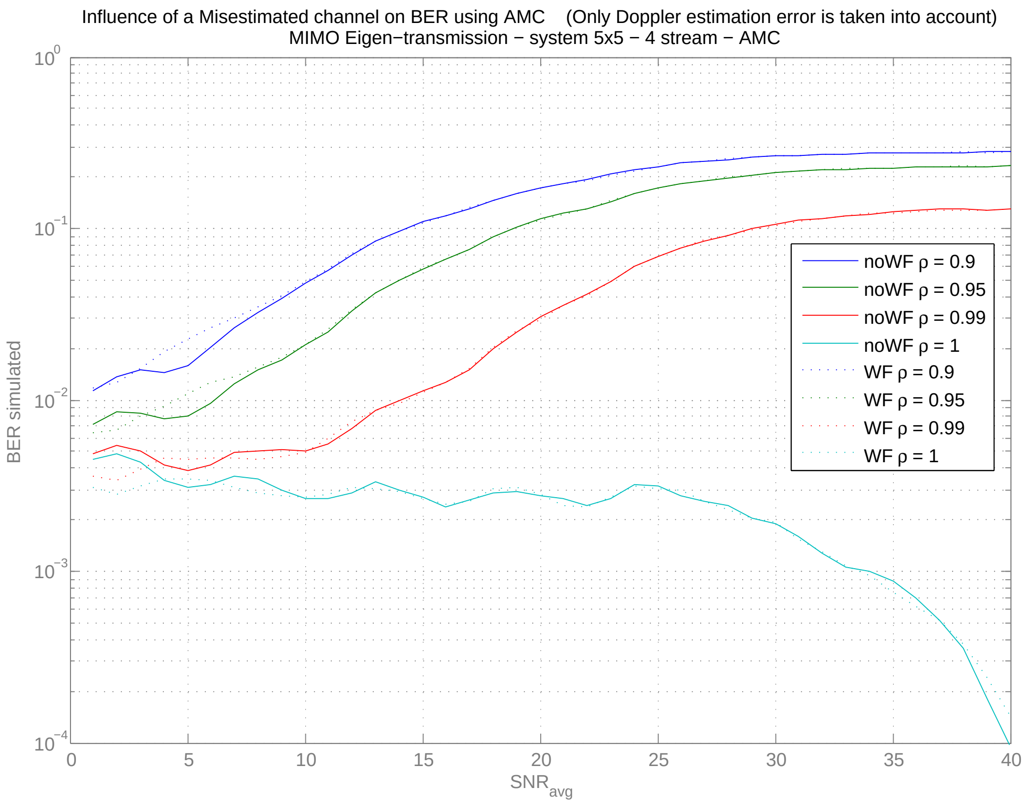

Figure 6.33: Influence of a misestimated channel (Doppler only) on AMC

Chapter 7

Conclusion

MIMO is a very recent topic in the telecommunications domain. It can be used with many different applications but is still in a constant state of research. Indeed, a wide range of researches are being led and publications have been and will be released regarding this subject. The concept of preprocessing is also very new and interesting, as MIMO pre-processing techniques will shape the future of communication systems.

This project was a very rewarding experience in terms of knowledge acquired and work completed. Indeed, we had very little background knowledge to understand the concepts involved in the modeling of a channel and the study of the influence of channel estimation errors on pre-processing mechanisms. Moreover, we did not use any external sources in the writing of the code that we performed using the software Matlab.

The learning of new concepts and their migration to code lines had us learn a lot. We started from theoretical equations that we had to understand and then input in the code, to later interpret the results and double-check them according to the theory.

The results we have reached taught us the importance of a good estimation of the channel in MIMO systems using Eigenmode transmission. Also, the Doppler effect has a tremendous influence on the transmission quality, especially at high frequencies. We were able to see how much resources the pre-processing required, mainly due to the use of the Singular Value Decomposition. Moreover, when it comes to interpreting the results, it is difficult to know how to present them, since anyone can choose a different context with system size, number of streams sent, modulations used...

Also, we are glad we managed to overcome our lack of knowledge and set a good working discipline that had us read through a lot of references and take the essential out of them, to later put theory stated into practice.

As a future work, we intend to run more detailed simulations (since some of them require a huge number of realizations to be accurate) and take a look back on the results interpretation.

Bibliography

[1] John G.Proakis and Massoud Salehi. *Comunication systems enginereering - second edition.* Prentice-Hall, 2002.

[2] Rohit Nabar Arogyaswami Paulraj and Dhananjay Gore. *Introduction to Space-Time Wireless Communications.* Cambridge, 2003.

[3] Andrea Goldsmith. *Wireless Communications.* Cambridge : Cambridge University Press, 2005.

[4] John G.Proakis. *Digital Communication - fourth edition.* McGraw-Hill, 2001.

[5] Andreas F.Molisch. *Wireless Communications.* WILEY and IEEE Press, 2005.

[6] Gilbert Strang. *Linear algebra and its application - third edition.* Saunders HBJ, 1988.

[7] T. S. Rappaport. *Wireless Communications, Principles and Practice.* Series Editor, 2002.

[8] Andersen J.B. Nguyen H.T. and Pedersen G.F. *Capacity and performance of MIMO systems under the impact of feedback delay*, volume vol.1. IEEE, september 2004.

[9] Huang H.C. Lozano A. Qinfang Sun, Cox D.C. *Estimation of continuous flat fading MIMO channels*, volume vol.1, Issue 4. Wireless Communications,IEEE, October 2002.

[10] T. Yoo and A. Goldsmith. *Capacity of fading MIMO channels with channel estimation error*, volume vol.2. IEEE Int. Conf. Commun., June 2004.

[11] S. Chung and journal = IEEE Trans. Commun. volume = vol.49 number = nř9 pages = 1561-1571 year = sep 2001 A. Goldsmith, title = Degrees of freedom in adaptive modulation: a unified view.

[12] Francesc Boixadera Espax and Joseph Jean BOUTROS. *Capacity considerations for wireless MIMO channels.*

[13] Inaki Berenguer. *Coding and Signal Processing for MIMO Communications.*

[14] Safa I. A. Ahmed and Kai-Kit Wong. *On the MIMO Capacity with Imperfect CSI.*

[15] Philippe Guguen. *Techniques multi-antennes émission-réciption, Applications aux réseaux domestiques sans-fil.* 2003.

[16] Jonghoon Ann; Yun Seok Choi; Yeonwoo Lee. *Performance evaluation and comparison of pre-equalizer for rain attenuation channels in a B-WLL uplink system*, volume IEEE 56th Volume 4. Kyun Hyon Tchah Vehicular Technology Conference 2002. Proceedings. VTC 2002-Fall, 2002.

[17] C.B. Peel. *Dirty-Paper coding*, volume IEEE Volume 20, Issue 3. Signal Processing Magazine, May 2003.

[18] EGGERS Patrick OPREA Alex KYRITSI Persefoni, PAPANICOLAOU George. *Time reversal techniques for wireless communications*, volume Volume 1. A. Vehicular Technology Conference ,26-29 Sept, vtc2004-fall. 2004 ieee 60th edition, 2004.

[19] Persefoni Kyritsi. *Waterfilling course.* Mobile Communication,Aalborg University,Denmark,2008.

[20] Persefoni Kyritsi. *MIMO and CSI course.* Mobile Communication.

List of Figures

List of Tables

Appendix A

Appendix

A.1 Narrowband versus Wideband models

A.1.1 Narrowband

Narrowband is the situation where the occupied bandwidth is small and the symbol time is long. We can neglect Inter Symbol Interference (ISI) if the symbol time is larger than the delay spread (approximately 10 times). It implies that the channel is sufficiently narrow that its frequency response can be considered flat. The message bandwidth will therefore be less than the coherence bandwidth of the channel. Even though no channel has perfectly flat fading, this assumption is very useful to simplify the analysis of wireless communication system. The following figure A.1 presents the transmission of the information of the channel. Depending on the channel model, the expression of the channel will vary and with it, the expression of the received signal accordingly.

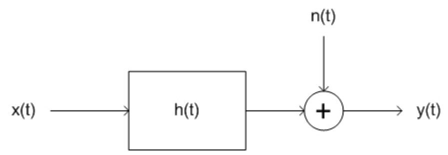

Figure A.1: Block diagram of the signal's transmission

The expression of the received signal is here:

$$y(t) = x(t) \otimes h(t) + n(t) \tag{A.1}$$

In a narrowband model, we consider that the channel frequency response is flat and the delays between each path are negligible. Thus, the channel can be expressed as:

$$h(t) = h\delta(t) \tag{A.2}$$

Using this in (4.5) , we obtain:

$$y(t) = h.x(t) \tag{A.3}$$

We have presented in Figure A.2 a binary sequence in a wideband situation and the consequence of multipath over the received stream. Frequency responses of the channel and the signal, with a symbol time larger than the delay spread are also displayed (2nd figure to add).

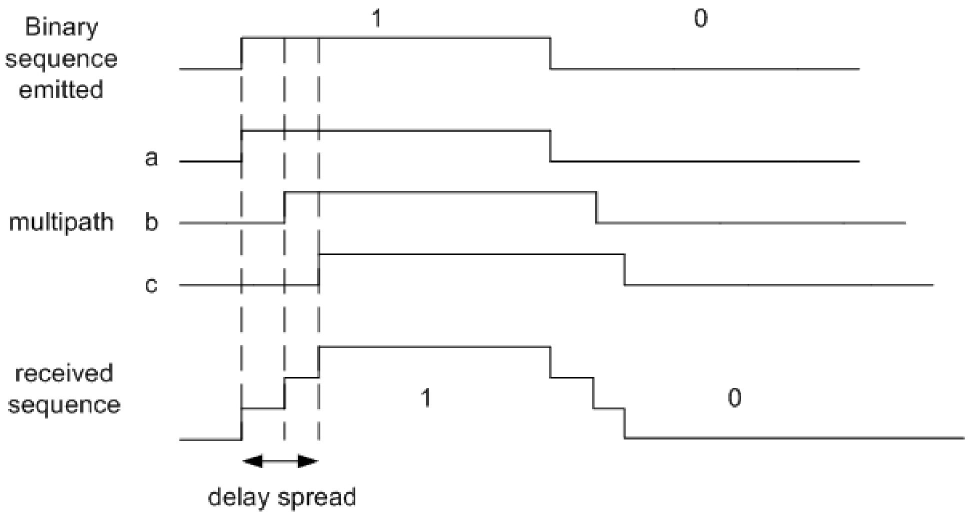

Figure A.2: Binary sequence sent and received in narrowband with multipath

We notice that it is easy to decipher the stream at the receiver end. The multipath effect is not that detrimental.

A.1.2 Wideband

A wideband transmission is at a higher bit rate than a narrowband one (i.e. the symbol time is smaller than delay spread). In this case, the message bandwidth is larger than the coherence bandwidth of the channel, and the channel response becomes frequency-selective. Also, the signal is unlikely to vanish completely in a deep fade, because its bandwidth is so wide that, no matter how bad the channel is at some frequencies, there will always be some components present where the channel is good. However, this also introduces the drawback of the wideband which is the presence of Inter Symbol Interference that needs to be handled. Indeed, the delayed paths here matter and are overlapping. We need to take them into account in the wideband channel equation. From the situation described in figure A.1, we have:

$$h(t) = \alpha_1\delta(t) + \alpha_2\delta(t - T_1) + \alpha_3\delta(t - T_2) + ... + \alpha_n\delta(t - T_n) \tag{A.4}$$

$$h(t) = \sum_{i=1}^{n} \alpha_n\delta(t - Tn) \tag{A.5}$$

Using this in (4.5), we obtain:

$$y(t) = x(t) \otimes \sum_{i=1}^{n} \alpha_n\delta(t - Tn) \tag{A.6}$$

We simplify:

$$y(t) = \sum_{i=1}^{n} x(t) \otimes \delta(t - Tn)\alpha_n \tag{A.7}$$

$$y(t) = \sum_{i=1}^{n} x(t - Tn)\alpha_n \tag{A.8}$$

Developping the sum, (A.8) becomes:

$$y(t) = \alpha_1 x(t) + \alpha_2\delta(t - T_1) + \alpha_3\delta(t - T_2) + ... + \alpha_n\delta(t - T_n) \tag{A.9}$$

The desired signal is included in the component $\alpha_1 x(t)$, the other unwanted components being the source of the ISI.

Figure A.3 shows a binary sequence in a wideband situation and the consequence of multipath over the received stream. Frequency responses of the channel and the signal, with a symbol time smaller than the delay spread are also displayed (2nd figure to add).

We notice that here it is very difficult to decipher the stream at the receiver end. The multipath effect is introducing ISI, the waves using different paths are interfering with each other as we can see on the received sequence.

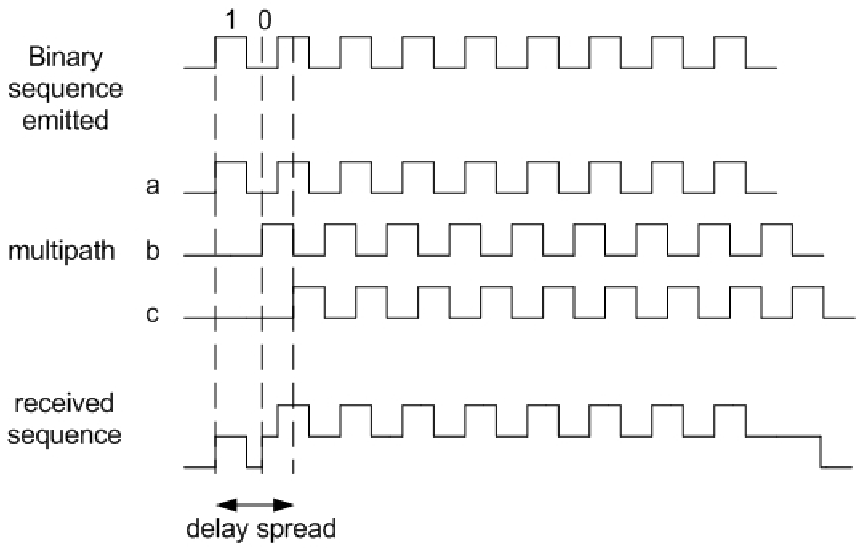

Figure A.3: Binary sequence sent and received in wideband with multipath